The influence of spatial variation on the design of foundations of immersed tunnels Advanced probabilistic analysis

't Hart, Cornelis Marcel Pieter; Morales-Nápoles, Oswaldo; Jonkman, Bas

DOI
10.1016/j.tust.2024.105624

Publication date
2024

Document Version
Final published version

Published in
Tunnelling and Underground Space Technology

Tunnelling and Underground Space Technology 147 (2024) 105624

Contents lists available at ScienceDirect

Tunnelling and Underground Space Technology

journal homepage: www.elsevier.com/locate/tust

The influence of spatial variation on the design of foundations of immersed tunnels: Advanced probabilistic analysis

Cornelis Marcel Pieter 't Hart [a,b,c,*], Oswaldo Morales-Nápoles [a], Bas Jonkman [a]

[a] TU Delft, Delft, The Netherlands
[b] Tunnel Engineering Consultants, Amersfoort, The Netherlands
[c] Royal HaskoningDHV, Amersfoort, The Netherlands

ARTICLE INFO

Keywords:
Immersed tunnels
Soft soil tunnels
Bedding
Covariance length
Dredging
Gaussian random fields
Vine Copulas
Non Parametric Bayesian Network

ABSTRACT

Immersed tunnels are positive buoyant structures during installation and negative buoyant after installation. A tunnel is composed of sequential immersed elements that are coupled to each other in joints. Tunnel elements consist of segments which are compressed to each other by longitudinal post-tensioning. After immersion the tunnel is supported by the seabed and the longitudinal post-tension is cut at the joints between segments. Therefore, the structure is a segmented lining which is sensitive for settlements due to non uniform circumstances over the length of the tunnel. An uneven response of the bedding underneath the tunnel introduce shear forces in joints of an immersed tunnel. Because immersed tunnels need to be buoyant during installation, they have limitations on weight and geometry, the size and therefore the capacity of these shear keys is limited because the height of the tunnel, as shear keys are applied in the walls of the tunnel. The foundation response is influenced by many factors related to subsoil but also to construction and dredging tolerances. The shear forces were derived as a function of different covariance lengths for subsoil stiffness and dredging tolerances for different tunnel layouts. In reliability analyses, using two different probabilistic methods, exceedance probabilities of maximum shear forces are derived for one lay out using Non Parametric Bayesian Networks and Vine Copulas. The analyses give more insight in to the magnitude of the shear forces in joints both in conditioned and unconditioned situations and this can be used for the design of immersed tunnels.

1. Introduction

Immersed tunnels (IMT) are tunnels supported by soft soil and a foundation layer acting as a bedding. The majority of this type of tunnels is constructed using prefabricated elements immersed to a trench in the seabed. After immersion and finalisation, the structure behaves as a segmented lining with segments of a length with about 20 to 25 m, that are connected with joints. Using this approach, the tunnel is less vulnerable for differential settlements as the segment joints only transfer shear forces via shear key constructions and large bending moments over the length of the structure are avoided. In the most common current design approach, an alternating bedding scenario (reduction of the stiffness on a single segment using a prescribed factor, as defined by Dutch requirements (RWS, 2017) and adopted for many tunnels worldwide) along the tunnel axis is used as a conservative approach. However it does not account for spatial variability in both the subsoil and the foundation of the tunnel. Instead, the current design approach is geometrically orientated on the tunnel to find the largest possible shear forces and not on the variability of the bedding support.

In this paper the authors present a method to find the variability of forces in the shear key using Gaussian Random Fields (GRF), which are parameterised by a covariance length. Next, the probability distribution of the force in the shear key is found by using two different probabilistic methods, Vine Copulas (VC) and Non Parametric Bayesian Networks (NPBN), in which the covariance lengths for the subsoil and dredging tolerances are related to the shear forces. Both methods differ but allow both for conditioning. These probabilistic methods are valuable and can be identified as scientific engineering, because they connect variability in subsoil and construction to estimate the forces in the shear key in both conditioned and unconditioned situations. Using these methods, both the GRF as well as a multivariate probability distribution for covariance lengths for (spatial variability of soil properties) and shear forces, will result in a complete characterisation of the probabilistic relation between support conditions and the shear forces in the tunnel to be used in design. Secondly, more efficient and more robust designs for immersed tunnels can be developed and can be identified as an alternative for the current design approach.

* Corresponding author at: TU Delft, Delft, The Netherlands.
E-mail address: c.m.p.thart@tudelft.nl (C.M.P.'t. Hart).

https://doi.org/10.1016/j.tust.2024.105624
Received 25 September 2023; Received in revised form 30 November 2023; Accepted 31 January 2024
Available online 4 March 2024

Nomenclature

Δt_{dl}	Dredging tolerance
Δt_{pl}	Gravel placement tolerance
μ	Mean value
Σ	Covariance matrix
σ	Standard deviation
σ_a	Average contact pressure
σ_b	Bedding response
A_b	Contact area underneath the tunnel
A_b	Bedding-tunnel contact area
F_i	Force at segment i
F_k	Absolute force at shear key
h_f	Foundation thickness
k_b	Bedding stiffness
k_f	Foundation material stiffness
k_s	Soil stiffness
L_{cov}	Covariance length [m]
L_i	Influence depth of the tunnel
n_x	Number of points in x direction
n_y	Number of points in y direction
X	Location
x_n	x-coordinate of point n [m]
y_n	y-coordinate of point n [m]

The demonstrated model and method in this paper also has limitations. For example, it assumes that the loads are uniform over the tunnel. Additionally, only 2 keys are considered per joint to transfer the shear forces, while in practice could be more. On the other hand, only 3 variables are considered in the probabilistic methods. This can be extended by other variables, such as spatial variability of the sediment height on the tunnel site. Furthermore, this method clearly differs from the current design approach. To use this method in design practice, engineers should have a more than basic understanding of the probabilistic tools employed.

After a brief literature overview, the paper handles first the concept of immersed tunnels as tunnel structures in soft soil, a brief introduction on GRF is given and the probabilistic concepts of VC and NPBN. The explanation of the method starts with the used model, its variations and specific conclusions on the relation between the covariance lengths and the force in the shear key. Based on the findings, the probabilistic analyses, using both methods, are conducted and the distribution of the shear force is found for both unconditional as well as for conditional situations. The paper is closed with conclusions and discussions as well as recommendations on follow-up research are given on improving and to overcome the limitations.

2. Literature overview

Different types of immersed tunnels (IMT) as well as their construction methods are discussed by Rasmussen (1997). A general description of the IMT construction technique and a historical perspective is given by de Wit and van Putten (2014) and design principles are described by Grantz (1997). A description of the development over the years is given by Glerum (1992).

IMTs have traditionally a foundation of a gravel or a sandflow foundation, both have their advantages and disadvantages, but differences between both methods were already described in 1978 by van Tongeren (1978) and scale model tests on sand-flow were performed and researched by Li et al. (2014). The sand-jetting or sand-flow, was applied, for example on the Maastunnel in 1942 (Gravesen and Rasmussen, 1993) and is highlighted by Glerum (1995). The gravel foundation was applied to the Øresund link between Copenhagen and Malmö.

Tunnels, not limited to IMT, rely on geotechnical as well as structural analysis. Random fields have been applied in a comparison study by Cheng et al. (2019) of a pressurised tunnel face of a bored tunnel and provides a practical design tool. Gong et al. (2018) presents a probabilistic analysis based on a random field generation for a longitudinal analysis for a bored tunnel. For a bored-tunnel section, a 2D plain strain approach including a random field generation is presented by Yu et al. (2019) in which the reliability of the tunnel lining is validated.

The application of spatial variability or (Gaussian) random fields is yet uncommon in designs of IMT foundations. Random fields are stochastic processes in space, or in other words, random functions over a given domain Adler and Taylor (2009), Hristopulos (2020). Random fields are used in many research areas, such as environmental engineering, social sciences, finance, astronomy and many others. Liu et al. (2019) shows the development in research of this random fields. Within the research in the field of civil engineering the application of GRF is frequently observed in geotechnical analysis for example for levees and embankments (Hicks and Li, 2018), Li et al. (2017) . The spatial variability of a soil continuum can be described using this method, see for example (Papaioannou and Straub, 2015; Soubra et al., 2008; Kasama and Zen, 2011). Besides the geotechnical applications, random fields are also used in structural mechanical cases. Bucher (2006) shows the application of it in material properties, such as the computation of modulus of elasticity or strength as well as for geometrical properties, like thickness in shell models. The application of random fields to trusses is researched by Bocchini (2008) and discusses the application in the reliability analysis of Cable Stayed bridges. In these examples the concept of random fields in Finite Element analysis is used. A description of this approach is given by (Vanmarcke et al., 1986).

In this study 2 different probabilistic methods are used, Non-Parametric Bayesian Networks (NPBN) and Vine Copula (VC). Both are graphical models and represent probabilistic dependence between the nodes. NPBNs are well described by Hanea et al. (2015). The NPBN in this research is implemented using the `Python` toolbox `BANSHEE` (Paprotny et al., 2020; Koot et al., 2023). NPBNs have been used in different fields of application such as hydrology (Paprotny and Morales Napoles, 2017) and flood risk (Paprotny et al., 2021; Couasnon et al., 2018). In order to assess of civil structures, NPBN are applied in Mendoza-Lugo et al. (2022), Morales Napoles and tno (2014), Morales-Nápoles and Steenbergen (2014) to model weight in motion data as result of traffic load. An application of this weight in motion model is used in Torres-Alves et al. (2022) in the reliability assessment of an submerged floating tunnel and in Mendoza-Lugo et al. (2019) to assess the reliability of bridges. VC can be used as a modelling tool for complex probabilistic dependency and used in many fields of application (Aas et al., 2009; Aas and Berg, 2009; Min and Czado, 2010; Chollete et al., 2008; Pouliasis et al., 2021; Jäger and Nápoles, 2017). Key in the application is to use a Regular Vine (RV) that represents fairly the data. With the increase of the number of variables in a dataset the number of possible unique Vine Copulas increases drastically as shown in Morales Napoles (2016) and Morales Napoles (2010). The combination of spatial variability and a probabilistic approach to estimate the shear key forces in immersed tunnels is a topic which is not addressed in literature.

3. Concepts

3.1. Immersed tunnels

Currently, the majority of IMTs are constructed using prefabricated elements of 100 to 150 m in a dry dock situation. The elements consist out of segments of 20 to 25 m which are compressed to each other for transportation by a post-tensioning system. After casting and post-tensioning the element, it is towed to the tunnel location and

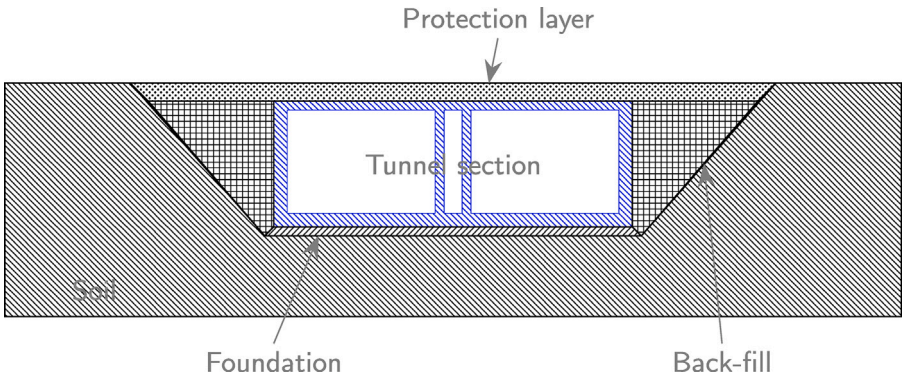

Fig. 3.1. Typical cross section of an immersed tunnel section.

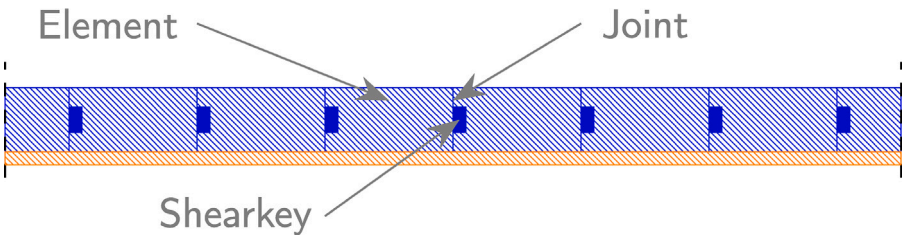

Fig. 3.2. Typical longitudinal section of an immersed tunnel section.

immersed into a dredged trench and laterally locked at its horizontal position using a back-fill and a protection layer (see Fig. 3.1). After immersion temporary post-tension is deactivated by cutting the tendons at the joints. As a result a continuous flexible system is created and at the joints shear forces need to be transferred between segments (see Fig. 3.2).

The shear keys, which connect the segments provide a vertical shear capacity. The capacity is dependent on the size and material of the key. Adjustment of the key has limitations. For example, as mentioned before, the tunnel needs to be buoyant in the construction phase, adding material like thickening the key will influence this process. Furthermore, the key itself is limited by the height of the tunnel. Considerations for other materials has financial consequences. At the shear key location, a flexible joint is constructed. Flexible joints are "weak" points in terms of water tightness of the tunnel and its amount should be limited. In the current design approach of alternating bedding scenarios, longer distances between joints will increase the forces in the shear key.

An optimal design would meet a segment length where the shear key is loaded to its maximum capacity. The results presented in this paper are based on an analysis of a rectangular tunnel section using a gravel foundation, although the same approach as presented here can be used for a sand-flow foundation. In current designs, a conservative approach using a single reduction parameter on a segment foundation is applied in an alternating bedding stiffness.

3.2. Gaussian random fields - spatial covariance

The spatial covariance indicates that a local value of a particular parameter is correlated with neighbouring values of the same parameter depending on the spatial distance between locations. The distance between two point dictates to what extent the values on the two location will vary. In this research GRF are applied to simulate the spatial variability. If a distance between 2 points increases, the covariance (statistical correlation) decreases exponentially. The covariance between two points in a grid is defined by the covariance length (L_{cov}) as expressed in Eq. (1), in the example with 0.5, 1 and 2, which shows these different covariances over the distance between points. To illustrate this dependency, for 3 hypothetical situations, three covariance length functions over distance have been plotted in Fig. 3.3. The actual covariance between individual locations is dictated by L_{cov}. If the covariance length is halved, the covariance between two points decreases faster; in contrast, if the covariance length is doubled, the covariance between two points decreases more slowly. If a surface is discretised to n_x times n_y in which n_x is the number of points in the longitudinal direction and n_y in the lateral direction, the total number of points n is defined as $n = n_x \cdot n_y$. The covariance matrix Σ contains the information regarding the covariance between all points within the grid defined by n_x and n_y. Factor $\frac{1}{2}\sqrt{\pi}$ in Eq. (1) is the scaling factor can be adjusted for model representation.

Table 3.1
Element characteristics.

Element length	[m]	varies
Element width	[m]	30.0
# segments	[–]	6
Segment length	[–]	20

If all distances between all points are available in a distance matrix, the covariance matrix Σ can be found in which for each connection the covariance is defined. Using Eq. (2) a multivariate Gaussian distribution be found and samples can be generated given L_{cov}. A sample of the field can then be transferred to any other distribution using a quantile transformation in which the quantiles of the normalised Gaussian distribution map to the quantiles of the target distribution. For the generation of GRF in this research, the `GSTools`, a toolbox for geostatistical modelling in `Python` is used (Müller et al., 2022).

The application of GRF is yet uncommon in designs of tunnel foundations. By nature, the soil parameters will develop continuously over the area. Special circumstances like faults and other exceptions will give raise to discrete transitions, but are not considered in this research. The trench is dredged to immerse the tunnel in it, by itself the dredging process has a tolerance. After dredging, a layer of gravel is applied to the required level. The soil variables, such as stiffness, and the dredging level, which is directly related to the thickness of the foundation layer (as presented in Fig. 4.2), are spatially correlated and

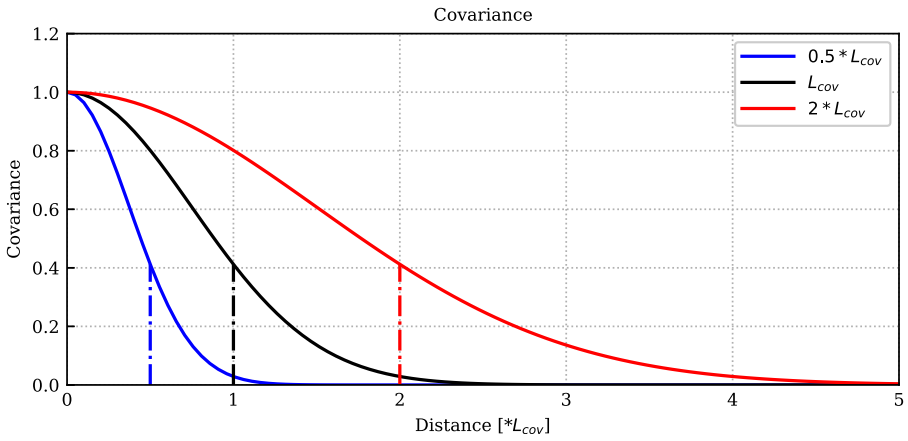

Fig. 3.3. Covariance based on covariance length.

can be described using GRF.

$$cov((x_1, y_1), (x_2, y_2)) = e^{-\sqrt{\pi}/2 \frac{\sqrt{(x_2-x_1)^2+(y_2-y_1)^2}}{L_{cov}}} \tag{1}$$

$$f_X(x_1, \ldots, x_n) = \frac{e^{-\frac{1}{2}(x-\mu)^T \Sigma^{-1}(x-\mu)}}{\sqrt{(2\pi)^n |\Sigma|}} \tag{2}$$

3.3. Probabilistic methods (Vine Copulas and non-parametric Bayesian networks)

In this research two probabilistic methods are used. Both, Non-Parametric Bayesian Network (NPBN) and Vine Copulas (VC), represent multivariate distributions along with their dependence structure. Both methods are quantified with a data-set which will be generated using the structural model of Section 4. The multivariate distributions are based on the 1-dimensional marginal distributions of individual variables and the interconnections between them describing probabilistic dependence. The distributions can be used to derive distributions of variables which on itself can be used for extreme value analysis. Additionally, distributions of a certain variable can be found for specific conditions on the other variables (so called conditional distributions) (see Table 3.1).

Non parametric Bayesian networks

A Bayesian Network (BN) is a graphical model that represent a joint distribution in a compact way. A BN consists of a *directed a-cyclic graph* (DAG) whose nodes represent random variables and arcs represent probabilistic dependence between the nodes. Here, we restrict ourselves to the class of NPBNs (Hanea et al., 2015). These class of BNs are based on copulas. A bi-variate copula C is a bi-variate distribution with uniform margins in [0,1]. More generally, a multivariate copula is a multivariate distribution function with uniform margins in [0,1]. One attractive feature of copulas is that they allow to separate the dependence from the influence of the margins. Many types of copulas are available and are described in detail in Joe (2014). In the NPBN framework, bi-variate Gaussian copulas are used to assemble the joint distribution. The bi-variate Gaussian copula is $C_\rho(u, v) = \Phi_\rho\left(\phi^{-1}(u), \phi^{-1}(v)\right)$ where $(u, v) \in \mathbb{R}^2$, ϕ^{-1} is the inverse standard normal distribution and Φ_ρ is the bi-variate Gaussian distribution with correlation coefficient ρ.

A NPBN is a BN where nodes are associated with a (typically) continuous random variable (X_i) with an invertible distribution function. Discrete random variables which preserve order may also be used in some cases. The direct predecessors of a particular node in the DAG are the "parents" of the "child" node. Arcs are directed from parents to children. The arcs of the BN are associated with (conditional) Gaussian copulas which are parameterised by (conditional) Spearman's rank correlations. Spearman's rank correlation coefficient is the usual Pearson's correlation coefficient computed with the ranks of the variates (instead of original units). For every node X_i with a non-empty, ordered set of parents $pa(X_i) = \{i_1, \ldots, i_p\}$, conditional rank correlations are assigned according to the following equation (3).

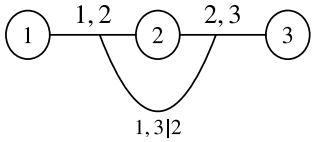

Fig. 3.4. Regular Vine with 3 nodes.

$$\begin{cases} r_{i,i_{p-k}} & \text{if , } k = 0 \\ r_{i,i_{p-k}|i_p,\ldots,i_{p-k+1}} & \text{for , } 1 \le k \le p-1 \end{cases} \tag{3}$$

Because of its construction, a rank correlation in [−1,1] can be assigned to any of the arcs of a NPBN. This assignment will lead to a valid rank correlation matrix. Once the NPBN has been setup, a unique joint distribution is determined. Using this joint distribution, efficient sampling is possible. Next to that, exact inference or conditioning (analytical updating of the joint distribution) is also possible given the copula assumption.

Vine Copulas

Equivalent to a NPBN a VC is also a graphical probabilistic model. A *Regular Vine* (RV) V on d elements (edge or nodes) is a sequence of trees $T_1, \ldots, T_{d-1}$ such that:

1. T_1 is a tree with node set $N_1 = \{1, \ldots, d\}$ and edge set E_1,
2. For $j \ge 2$, T_j is a tree with node set $N_j = E_{j-1}$ and edge set E_j
3. For $j = 2, \ldots, d-1$ and $\{a, b\} \in E_j$ it must hold that $|a \cap b| = 1$.

Property 3 is often referred to as the *proximity condition* which ensures that if there is an edge e connecting nodes a and b in tree T_j, $j \ge 2$, then a and b (which are edges in T_{j-1}) must share a common node in T_{j-1}. Thus, a regular vine on d elements is one in which two edges in tree j are joined by an edge in tree $j+1$ only if these edges share a common node in tree j. For $e \in E_j$, $j \le d-1$, the *constraint set* associated with e is the complete union U_e^* of e, that is, the subset of $N_1 = \{1, \ldots, d\}$ reachable from e by the membership relation.

For $j = 1, \ldots, d-1$, $e \in E$ if $e = \{i, k\}$ then the *conditioning set* associated with e is $D_e = \{U_i^* \cap U_k^*\}$ and the *conditioned set* associated with e is $\{C_{e,i}, C_{e,k}\} = \{U_i^* \setminus D_e, U_k^* \setminus D_e\}$. Note that for $e \in E_1$, the conditioning set is empty. Note as well that the order of an edge is the

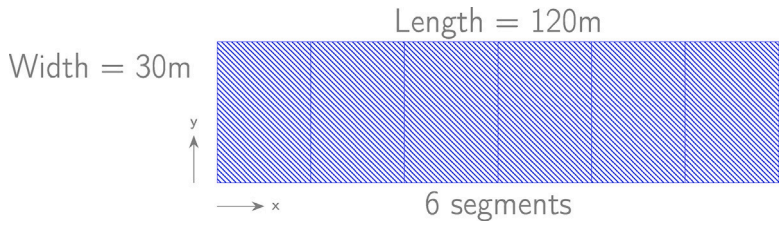

Fig. 4.1. Covariance length validation model - topview.

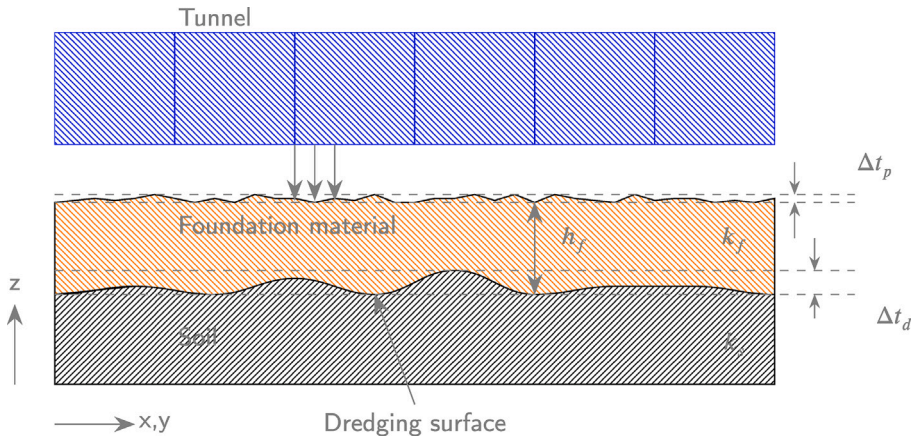

Fig. 4.2. Bedding definition (cross-section).

cardinality of its conditioning set. For $e \in E_j$, $j \leq d-1$, $e = \{i,k\}$ we have $U_e^* = U_i \cup U_k^*$. Thus, nodes of T_1 reachable from a given edge via the membership relation are elements of the constraint set of that edge. When two edges in T_j are joined by an edge in T_{j+1}, the intersection of the respective constraint sets forms the conditioning set. The symmetric difference of the constraint sets is the conditioned set of this edge. An example of a RV with 3 nodes is presented in Fig. 3.4.

In this study, only three variables are used; Covariance length for soil stiffness, covariance length for the dredging depth and the maximum shear key force found. There are only 3 possible RV with 3 nodes. Hence, a brute-force method is used to find the best regular vine to describe the data. The selection of best VC is based on the minimum Akaike Information Criterium (AIC) score.

For the fit, only the copula families with one parameter are used, including their rotated versions where applicable (Gaussian, Clayton, Gumbel, Frank and Joe). For this analysis the package `pyvinecopula` (Vatter and Nagler, 2022) is used, which is a `Python` interface to a library for Copulas based on `Eigen` (Guennebaud et al., 2010) which provides high performance implementation for inference algorithms for vine copula and bi-variate copula models.

4. Model and analysis

In order to research the influence of the covariance length of both the subsoil and the dredging depth, an artificial representative model is constructed. An IMT is supported by a bedding, consisting out of a subsoil and the foundation, and loaded with various loads acting on the tunnel. These loads will result in a bedding reaction underneath the IMT. The IMT is a concrete structure and has a significantly higher stiffness than the soil bedding. As a result, the force distribution of the tunnel segment itself will be insensitive to bedding variations. Flexibility is induced to the tunnel in the longitudinal direction by the segments joints and the immersion or element joints.

A base model of as a part of an IMT is used. The model has a length of 120 m and a width of 30 m (as specified in Table 3.1. The segments are equally distributed over the length of the element and have individual segment lengths of 20 m (L_s). A schematic overview is presented in Fig. 4.1.

The six segments of the IMT are assumed to have a constant vertical displacement over the length of the considered tunnel part. The segments are considered as rigid bodies and the joints as flexible. Fig. 4.3 shows the loading principle of the tunnel in the longitudinal direction.

The bedding is assumed to be elastic, but because of the spatial variability not constant over the contact area of the tunnel. The linear stiffness of the subsoil is derived by a geotechnical[1] analysis and the bedding stiffness is than based on the following parameters (see Fig. 4.2):

- Thickness of the foundation material (h_f in m).
- Stiffness of the foundation material (k_f in $\frac{\mathrm{N}}{\mathrm{m}^3}$).
- Dredging tolerance (Δt_d in m).
- Placement tolerance (Δt_p in m).
- Subsoil stiffness (k_s in $\frac{\mathrm{N}}{\mathrm{m}^2}$).

$$k_b = \frac{1}{\frac{1}{k_s} + \frac{h_f}{k_f}} \tag{4}$$

In the final situation, after immersion and after applying the soil cover, an average compressing pressure is supplied to the foundation underneath the tunnel (σ_a). The distributed load, on and in the tunnel, is adjustable by adding ballast weight and is based on vertical stability requirements. These requirements specify the minimal total resulting downward force to prevent floating up due to the buoyancy force. Because the bedding stiffness varies underneath the tunnel, the bedding response (σ_b) and therefore the load on the tunnel will vary as presented in Fig. 4.4. In this study, the vertical position of the tunnel is prescribed and adjusted in an iterative process until the average responsive stresses over the contact area A_b equals the load as described in Eq. (5). It is assumed that the total element will have the same vertical displacement and remain undeformed, this is a conservative approach.

[1] A separate geotechnical analysis is required to derive the subsoil stiffness based on the geological layers, the soil characteristics and the influence depth of the tunnel.

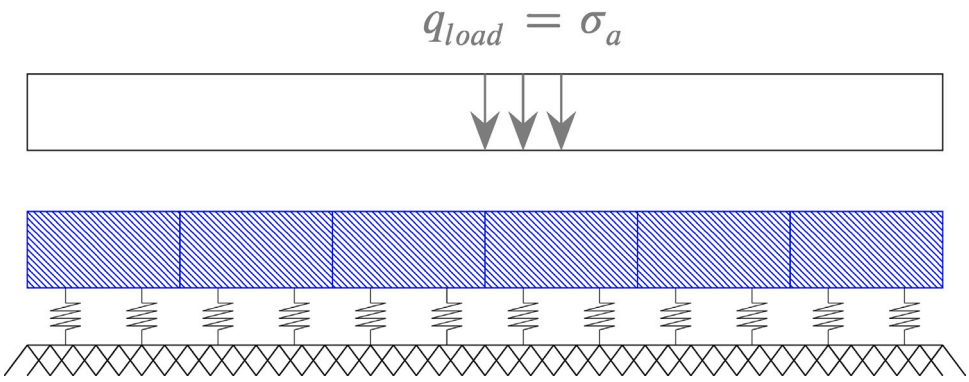

Fig. 4.3. Tunnel system.

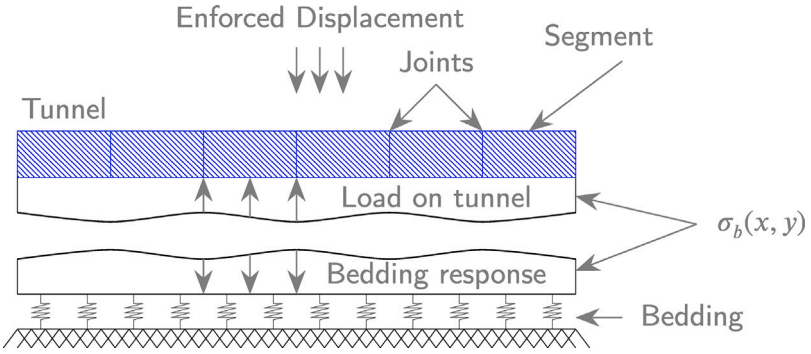

Fig. 4.4. Tunnel response.

In reality, the tunnel will deform slightly by small rotations of the segment and in the joints and, as a consequence, stresses will distribute between segments. If the stresses will redistribute, consequently the shear forces will reduce.

$$\sigma_a = \frac{\iint \sigma_b(x, y) dx dy}{A_b} \tag{5}$$

The bedding response variation leads to different stress distributions on the different segments. A shear force in a joint can be derived between two segments. Assuming the stiff IMT, the stresses will not redistribute between segments underneath the IMT and the maximum shear forces between segments will be found. In this study an IMT with a two shear key layout in the outer walls is assumed and each segment has therefore four shear keys. The sequence to derive the shear forces at a shear key after finding the equilibrium of the bedding response is presented in Fig. 4.5 and is obtained by:

- Integration of stresses underneath each segment to get the total force on a segment (F_i).
- Find the centre of gravity of the total force (red dots).
- Distribute the force to the shear key locations linearly (green dots).
- Define the shear key force as the absolute difference in forces between segments at the shear key locations ($F_{k,2-3}$ and $F_{k,1-4}$).
- Find the maximum shear key force of all shear keys.

In design, the maximum shear key force is used to compile a reinforcement layout for the shear key. In Section 5 this sequence is repeated for both different covariance lengths and different geometrical tunnel layouts and is the covariance length related to the shear key force. With this method, a spatial variability of the bedding stiffness underneath the tunnel is considered. The variability not only differs in longitudinal direction of the tunnel but also in the lateral direction. In the presented model, only a spatial variation in subsoil stiffness and dredging depth are considered, besides that, the model also considers non spatial correlated variations such as variations in the top surface of the gravel and in the gravel stiffness. More parameters, spatial or non spatial variated can be considered in the model, such as settlements over time and gravel placement equipment.

The model serves 2 different goals, the first one (Section 5.1) is to present the influence of the covariance length on the shear forces for different segment lengths. Secondly in Section 5.2, the structural model is used to gather a data-set to create a NPBN and RV. With these probabilistic models multivariate probabilistic analyses can be conducted and interactions between variables can found. As a result, probability distributions of variables, in this case the shear force, can be found to conduct extreme value analyses.

5. Results

5.1. Spatial variability

In this section, Monte Carlo analyses ($n = 1000$) are conducted in which the covariance lengths for both the soil stiffness as well as for the trench dredging are considered to be equal and fixed in each analysis. The generation of the variability of the subsoil stiffness and dredging depth are independent. An even more stronger effect would have been found if the same GRF was used for both parameters, but this was considered as less realistic as independent generation. In reality not only the variability will be independent but also the covariance lengths of both parameters will be independent. However to find a relation between covariance lengths and the shear key force, both are kept equal. Using this approach the distribution of the shear force given the covariance length. In Section 5.2, the covariance lengths are considered independently. For the bedding variations the variable distributions as described in Table 5.1 are used. These parameters are artificial and based on experience in several designs of various tunnels. In order to demonstrate the method, the quantity of the parameters is important as long as they are representative. For each sample, GRF are generated

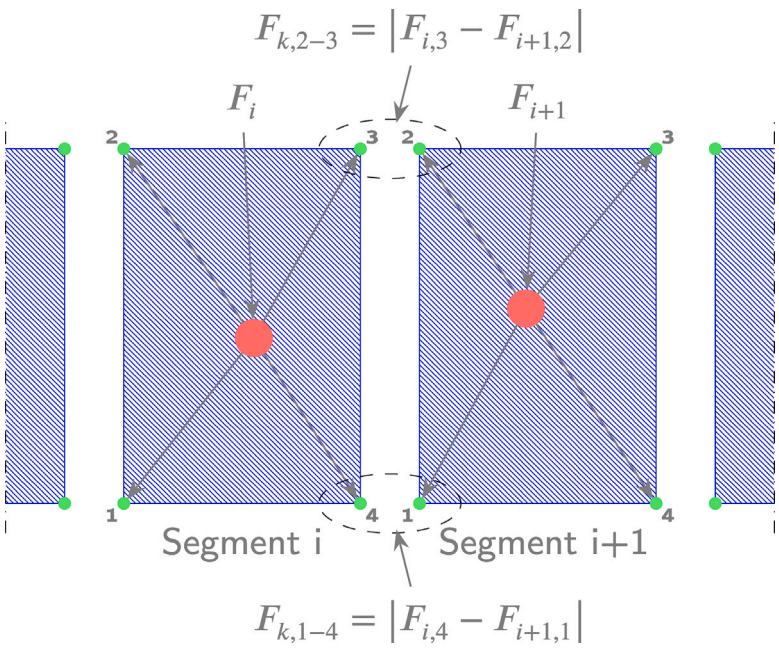

Fig. 4.5. Force at shear-key.

Table 5.1
Parameters and distributions.

Item	μ	σ	Distribution	Remarks
Gravel stiffness [kPa]	2000	300	Truncated Gaussian	uncorrelated min = 1000 max = 3000
Soil stiffness [kPa]	5000	1600	Truncated Gaussian	min = 1800 max = 8200 L_{cov} = varies
Trench dredging/Gravel thickness [m]	0.7	0.15	Truncated Gaussian	min = 0.35 max = 1.05 L_{cov} = varies
Gravel placement tolerance [mm]	0		Triangular	uncorrelated min = −10.0 max = 15.0

for both the subsoil stiffness as well as the thickness of the foundation layer based on the considered covariance length. The size of the GRF corresponds to the dimensions of the basemodel as shown in Fig. 4.1. Using the sequence specified in Section 4, the maximum shear key force can be found in each sample of the analysis and the total set result in a distribution of the maximum shear key force for a specific covariance length. The results are presented in Figs. 5.1–5.3. The following aspects can be identified:

- The maximum shear key forces (up to 4.8 MN) can be found if the covariance length is similar to the segment dimensions and the variation is larger.
- If the covariance length is small or large compared to the segment length, the maximum shear key force is small (with 1 to 1.5 MN) and shows a low variation.

In Fig. 5.3 the relation between the shear key force at the 95th percentile of the distribution and the covariance length is shown. The 95th percentile is chosen as the characteristic design force (in design considerations for ultimate limit state evaluation this value is multiplied by a partial factor (European Committee for Standardization, 2002)).

In Fig. 5.1 the number of segments and the width of the tunnel are considered to be constant. In Fig. 5.4 the segment length L_s is varied from 10 to 60 meter, while keeping the number of segments equal to 6 (which changes the total element length), so the total contact area under tunnel varies with the different segment length. On the horizontal axis the covariance length is divided by the segment length for comparison. The results are plotted for the covariance length over the segment length and the shear key force found at the maximum density as presented in Fig. 5.1. Fig. 5.5 shows the same figure as Fig. 5.4, but for comparison, F_k is divided by the contact area under the segment. All individual graphs are presented in Appendix A. The following observations can be identified from Fig. 5.4:

- F_k increases with the segment length L_s. Larger integration areas, due to the increase of L_s, underneath a segment will cause higher shear forces which can exceed the capacity of a shear key.
- The maximum F_k is found if the segment dimensions (length and width) and L_{cov} are similar.
- If L_{cov} increases to larger values compared to L_s, the F_k decreases.

There appears a strong relation between the covariance length and the shear key force. Secondly, as a geometrical consequence of a lower area below the segment, lower segment lengths show lower shear key forces. An optimisation of the segment length could be discussed, as joints are weaker spots in terms of water tightness. But in reality the segment length depends on other factors as well, such as the casting sequence, seasonal temperature loads introducing longitudinal effects and so on. However, the conclusion gives useful input in the early stage of the design of the geometry and structural solutions.

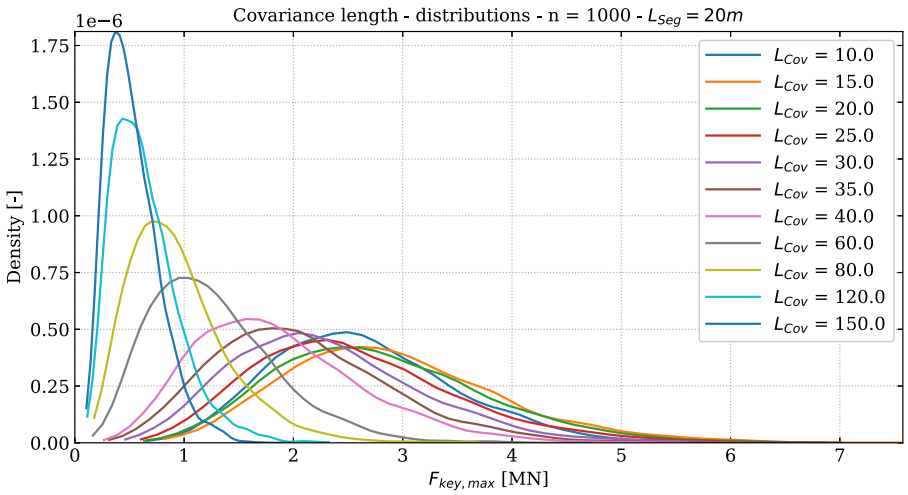

Fig. 5.1. Distributions of the maximum shear key force for different covariance lengths.

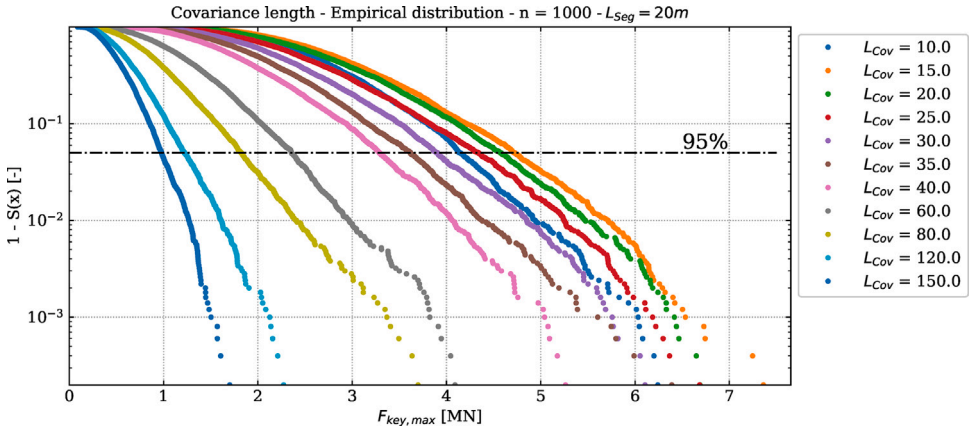

Fig. 5.2. Exceedance probabilities of the maximum shear key force for different covariance lengths.

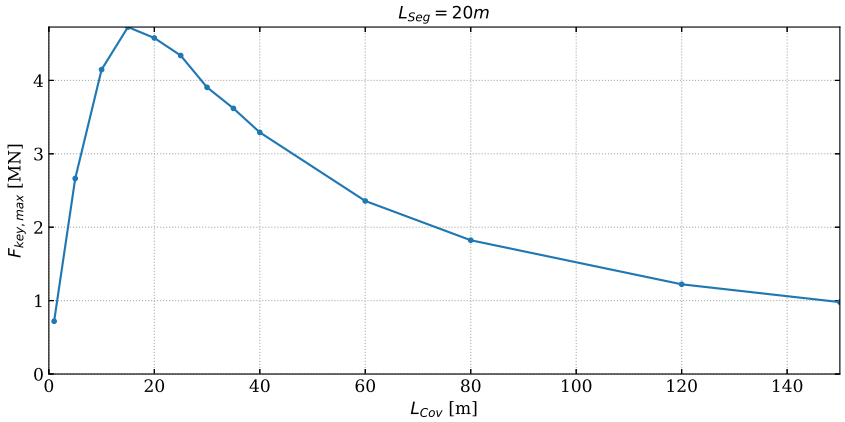

Fig. 5.3. Shear key force at 95th percentile as function of the covariance length.

5.2. Probabilistic analysis

Probabilistic models

Fig. 5.3 shows the relation between the shear key force and the covariance length for a length segment of 20 m. The maximum shear key force is found at a covariance length of about 15 m. From the figure, it can be concluded that there is a positive correlation between the covariance length and the shear key force up to a covariance length of about 15 m and a negative correlation for covariance lengths larger than 15 m. Rank correlations, which are often used to parameterise multidimensional models in statistical analysis fail to capture non-monotonic behaviour such as the one described in Fig. 5.3. Therefore, the model is split up into two parts. The correlation length on which the model is split is found by additional analyses between the interval of 10 m to 24 m with an increment of 2 m. For this interval a quadratic interpolation is derived to find the maximum value, which appears to be 16.3 m, as presented in Fig. 5.6. The data-set is split into two parts at this value an result into two separate data sets at the split value, the

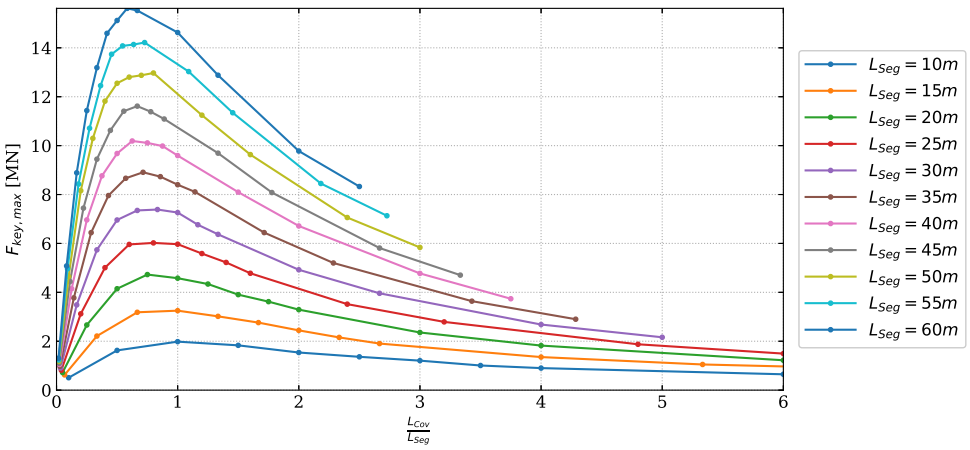

Fig. 5.4. Shear key force at 95th percentile as a function of the covariance length for different segment lengths.

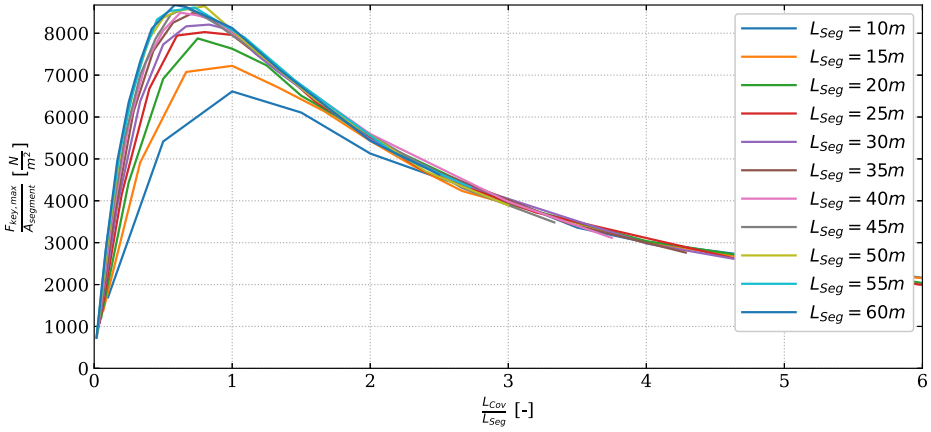

Fig. 5.5. Relative shear key force at 95th percentile as a function of the covariance length for different segment lengths.

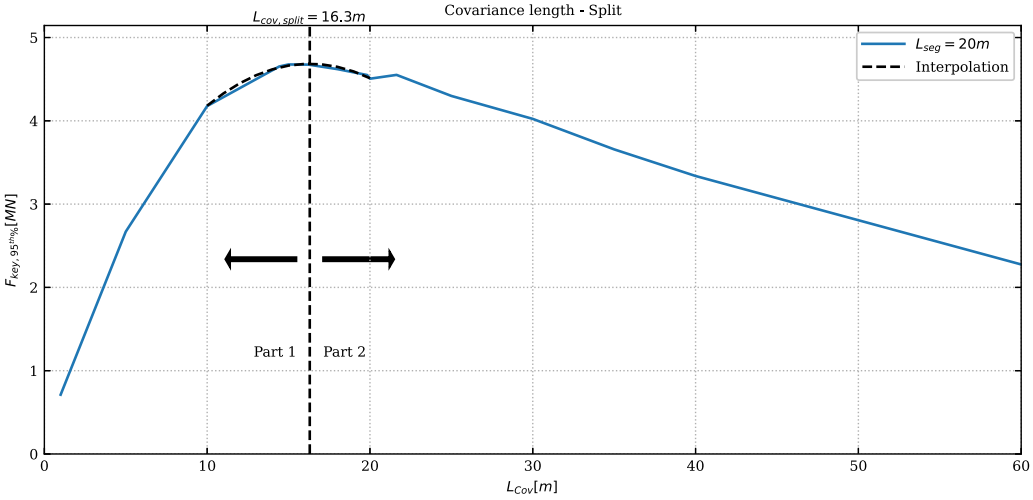

Fig. 5.6. Shear key force at 95th percentile as a function of the covariance length - splitted.

lower part (part 1) containing covariance lengths up to 16.3 m and the upper part (part 2) containing covariance lengths of 16.3 m and larger. Both parts show similar exceedance probability distributions. As this probabilistic approach focus on the maximum shear key force, it can be either conducted from part 1 and part 2. In Appendices B and C contain the results for both parts, in this chapter only part 1 is presented as the methods are equal for both parts.

The data for the Probabilistic analysis is generated using the base model in a Monte Carlo simulation ($n = 3000$). The covariance lengths were independently uniformly distributed between 0 m and 16.3 m and the total data contains 3 variables: the both covariance lengths and the maximum shear key force. The fitting is conducted by a `Python` package `SciPy` (Virtanen et al., 2020) using the most common distributions. The best fitted distributions are selected based on lowest sum of the square error between the observed value and the value

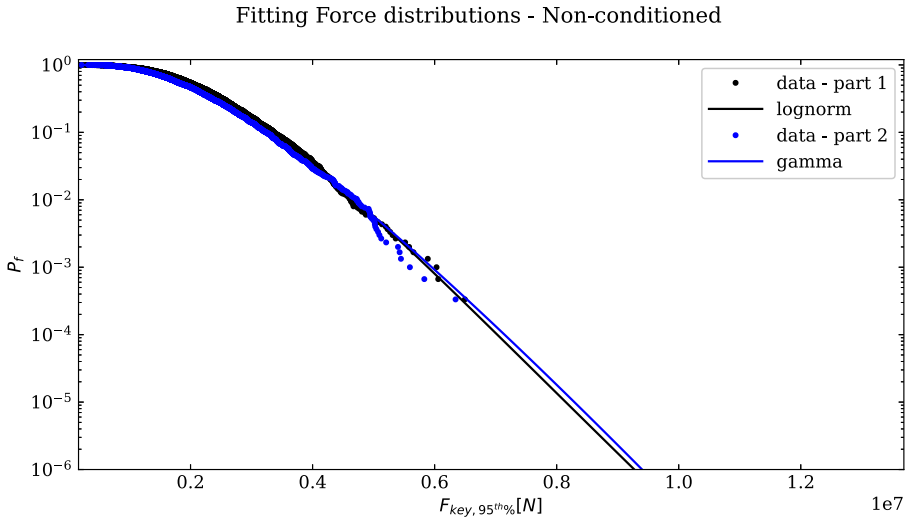

Fig. 5.7. Cumulative distribution function of shear key force at 95th with the best fit for both parts.

Table 5.2
Empirical rank correlation matrix for part 1 (lower).

	$L_{cov,soil}$	$L_{cov,trench}$	F_{key}
$L_{cov,soil}$	1	0.006	0.355
$L_{cov,trench}$	0.006	1	0.426
F_{key}	0.355	0.426	1

Table 5.3
Best fitted VC.

Tree 1:	Copula	Parameter
$L_{cov,soil}$ - Force	Gaussian	0.37
$L_{cov,soil}$ - $L_{cov,trench}$	Joe	1.01
Tree 2:		
$L_{cov,trench}$ - Force | $L_{cov,soil}$	Gumbel 180°	1.46

based on the distribution. For this analysis, the area of interest is at the tail of the data and it appears that the log-normal distribution fits best for part 1 (and the gamma distribution for part 2), as presented in Fig. 5.7. The parametric distribution for the shear force will used together with uniform distributions for the covariance lengths in the simulations using the NPBN approach to find probability distributions.

A unique joint distribution between the covariance lengths ($L_{cov,soil}$ and $L_{cov,trench}$) and the shear force is determined. In Table 5.2 the empirical rank correlation matrix is presented. The matrix show only a small correlation between covariance lengths as these are considered independent. The correlation between the shear key force and the shear key force are 0.36 to 0.43.

Using the rank correlations a NPBN is constructed with 3 nodes, representing both covariance lengths and the shear force, and 2 arcs, representing the correlation between the force to each of the correlation length. The NPBN is presented in Fig. 5.8 and the conditional rank correlation matrix is presented in Table B.2.

In order the validate whether the Gaussian copula represents the bi-variate pairs closely, a diagnostic tool is used. Appendix B contains the validation of the NPBN. The Cramèr-von Moses statistic, which is related to the sum of square differences between the empirical copulas and the parametric copulas is used. Fig. B.2 show the results of this validation. The graphs indicate, by the relative small differences, that the Gaussian copula (maximal 0.2) is a fair representation of the bi-variate distribution.

Fig. B.3 present the empirical cumulative density of the d-calibration scores, based on the Helliger distance (Morales-Nápoles et al., 2014). The d-calculation scores are the distance between empirical and empirical normal rank correlation, and the empirical normal and the normal rank correlation matrices. If these matrices are equal, the d-calibration score is 1. For both parts, the d-calibration score is within the uncertainty bounds if respectively 5000 and 25000 samples are drawn.

The full output for the probabilistic approach using VC is presented in Appendix C. For 3 nodes, only 3 different RV are applicable. The differences in AIC between the three possible RV are small, less than 5. The best fitted RV for part 1 is presented in 5.3 and has an AIC score of −1261. In the overview in C.2 small tail dependency can be observed.

As stated, the VC approach uses different copulas and is able to account for tail dependency. In Fig. C.2, the joint plot of the results is presented. In this graph tail dependency is visible. In the VC with the smallest AIC score for both parts, although the correlation is not strong with 0.35 to 0.43, tail dependent copulas are found. Compared to the NPBN approach, in which is concluded that the Gaussian copula give confident predictions of the dependencies, it is also seen in the CVM scores that the Gaussian copulas can be used, but that in some cases the tail dependent copulas show a slightly better score. Based on these findings and assumptions for both approaches, the VC approach is better while the results are still comparable.

Conditioning

With the best found models for both NPBN and VC, simulations are possible. A next step in the process is to condition the simulations. If inference or conditioning is applied to the models, an uncertainty distributions of remaining unknown nodes can be determined given a condition on one or more of the remaining nodes. In practice this is valuable, if a certain variable is deducted from field research such as CPTs or by applying measures to reduce the tolerance on dredging, the influence on the shear key force can be found and be accounted for in the design or the design can be optimised based on these findings or measures. It is also possible to use an opposite objective. So, conditioning on the shear force in this matter is also possible. That

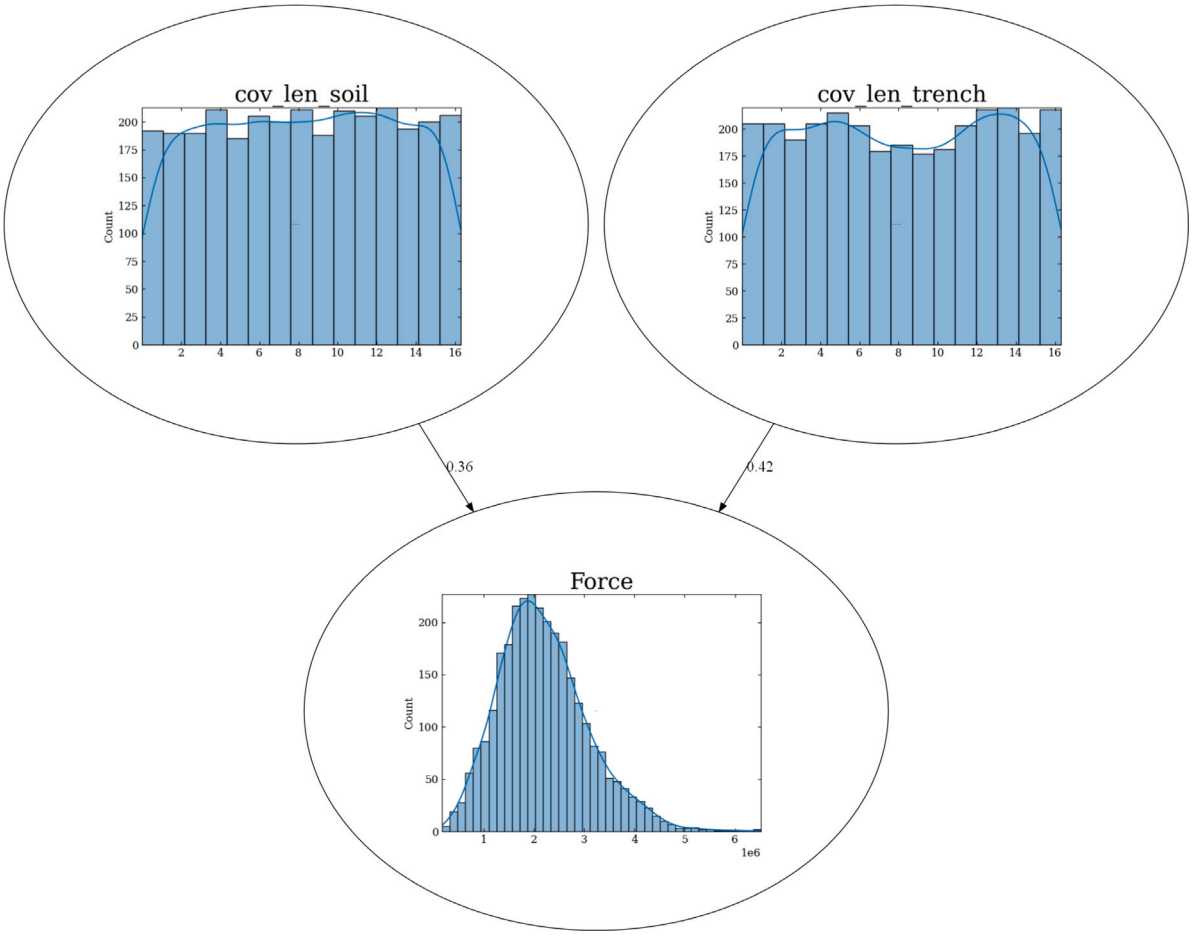

Fig. 5.8. NPBN - part 1.

will give the engineer the distribution of the covariance lengths of the soil stiffness and the dredging depth given a certain shear force.

In this research, the distributions are compared between the non-conditional distribution and different conditional situations. For both models, the lengths have been conditioned on different lengths. Next to the conditioning of the lengths, also the shear force has been conditioned, giving the following scenarios:

- Covariance length conditioned on 16.2 [m], 0.1 [m] from the split value.
- Covariance length conditioned on 8.15 [m].
- Only one covariance length conditioned on 16.2 [m].
- Only one covariance length conditioned on 8.15 [m].

The outcome for the shear force of the simulations of the RV is limited to the maximum value of the original data-set. However, a difference between NPBN and VC is that in the NPBN the fitted distribution functions have been applied while in the VC simulation, the outcome is based on the simulation data. As a consequence, a dataset is created using the best fitted RV ($n = 1E7$) and a conditional dataset for RV is conducted by specifying a small interval around the conditioned variable (in this case 0.2 m) and select a sub-dataset from the total simulation data based on this interval (or intervals if applicable, if conditioned on more variables).

In Appendix B.2 and B.4 conditional exceedance probabilities are presented together with the unconditioned results for the NPBN and in Appendix C.2 and C.4 the equivalent results for VC are presented.

In general, the results slightly differ between the NPBN and the VC. Main differences in the approaches of both methods are already specified in the previous sections. In Table 5.4 the uncertainty distribution for the forces have been derived based on fitted distributions. If the conditioning of one of the covariance lengths is 16.2 m, the shear forces increase compared to the original dataset and when the lengths are conditioned to 8.15 m the forces decrease. If the conditioning for the 16.2 m cases are compared, it can be observed that in case both lengths are conditioned, the forces are larger than when only one length is conditioned. Both observations are validated by the findings in 5.1. The difference between the covariance length for the subsoil and for the trench are compared, the forces are higher in case the covariance length for subsoil is conditioned. It can be concluded that the influence of subsoil stiffness on the bedding is larger trench depth (and the related thickness of the foundation layer). However, this is case specific, if the thickness of the layer differs and the stiffness of the subsoil stiffness differs, the conclusion can be otherwise.

Additionally, for NPBN also conditioning have been conducted on the forces. Using approach, the probability distributions for the covariance lengths can be derived. The method is equal as for the conditioning on the covariance lengths, as described previously. Fig. B.7 show the probability diagram for the covariance lengths when the shear force is conditioned. The black line in the diagrams show the distribution from the original sample, the other lines show the distributions for a conditioned shear force of 2.0 MN (blue), 5.0 MN (green) and 7.0 MN (red). In all graphs the blue line is below the black line, which indicates

Table 5.4
Shear forces in [MN] for different conditions.

	Original dataset	Conditioned on 2 lengths L = 16.2 [m]		Conditioned on 2 lengths L = 8.15 [m]		Conditioned on $L_{corr,soil}$ = 16.2 [m]		Conditioned on $L_{corr,soil}$ = 8.15 [m]		Conditioned on $L_{corr,trench}$ = 16.2 [m]		Conditioned on $L_{corr,trench}$ = 8.15 [m]	
		NPBN	VC	NPBN	VC	NPBN	VC	NPBN	VC	NPBN	VC	NPBN	VC
1.00E−02	4.70	7.35	6.90	4.14	4.05	6.07	5.93	4.32	4.45	5.73	5.67	4.47	4.40
1.00E−03	5.89	8.73	8.05	4.98	4.84	7.34	7.12	5.24	5.49	6.92	6.83	5.46	5.35
1.00E−04	7.03	10.02	9.09	5.73	5.56	8.53	8.20	6.07	6.48	8.00	7.87	6.37	6.22
1.00E−05	8.15	11.27	10.06	6.43	6.23	9.69	9.21	6.85	7.45	9.01	8.84	7.22	7.04
1.00E−06	9.27	12.49	10.98	7.09	6.87	10.84	10.17	7.59	8.41	9.98	9.77	8.03	7.82

that the probability of the covariance length is not close to the split value. In contrast, the green and red lines are above the black line. The probability that the covariance length is closer to split value is higher than in the original sample. The red lines indicates that when a shear force of 7.0 MN is conditioned, a covariance length closer to the split length is more probable than in case of a shear force of 5.0 MN (green line). With this perspective, the designer has an option of a different objective and use the capacity of the shear key as a starting point. If the covariance lengths of subsoil can be derived, the design can be adjusted to the circumstances.

6. Relation to traditional design

In the more traditional design approach with the alternating bedding, the stiffness is considered uniform underneath a segment and a segmented beam on an elastic foundation is used to describe the model behaviour. To account for torsional effects and consequently varying shear forces in the keys in one joint a factor is used which usually is taken as 20% to 25%. Variation of the bedding along the tunnel is accounted by an alternating bedding which is specified by a factor depending on the foundation method. In the alternating bedding approach, no spatial variation in the subsoil is considered and is independent of the dredging method. In reality, this will vary by method and consequently by the marine environment and depth.

The method presented in this paper varies substantially from the current design approach. In that approach, the tunnel is modelled in a 2D space. Both methods require soil investigation and interpretation of these results. If the soil investigation is intensified, both models will have an increasing accuracy but only on the subsoil stiffness. Nevertheless, if a covariance length or an interval of covariance lengths can be derived, subsequently a distribution of shear forces can be derived using conditioning on this extended knowledge. In case the covariance length cannot be derived based on the available soil investigations, an upper bound for the covariance lengths can be found in estimation of the split value of the covariance length. Conditioning on an interval on this value will give an upper bound distribution of shear forces.

In Eurocode (European Committee for Standardization, 2002) and the ROK (RWS, 2017), the design is based on the Load Resistance Factor Method (LRFM). In short, in this method, the probability on both forces as well as that of the resistance are accounted for by partial factors. For the service limit state (SLS) the loads are applied in frequent combinations and for the ultimate limit state (ULS) the loads are combined and multiplied by a partial load-factor. These load-factors differ for different load cases. The limits states together will result in a "frequent" load and a maximum considered load. These are in fact 2 quantiles in a load distribution. Where the SLS can be considered as the mean value and a characteristic value at the tail of the distribution. In the presented method using representative loading, a distribution of the shear force is found, which can be equivalently considered. For the SLS, which focuses on durability in design, the mean or 50^{th} quantile of the distribution can be used. In ULS design, which focus on the structural capacity, the force can be found by selecting the quantile which relates to the required reliability index for the tunnel.

7. Conclusion and discussion

In this research a method is presented to establish a relation between spatial variation of subsoil and dredging parameters and the shear key forces in IMT and find exceedance probabilities using Non-parametric Bayesian Networks and Vine Copulas. Considering the relation between the covariance lengths and the shear key forces, the following conclusions can be drawn:

- If the covariance length is in the same order as segment length of the tunnel, the largest shear forces will be found.
- The absolute shear key force increases with the segment length.

The latter conclusion is obvious, the area of a segment over which the stresses are integrated is larger and will lead to larger forces. Based on these conclusions, the design of the segment length can be optimised if the covariant lengths are known or estimated within limits, for example by more intensive soil investigation using CPT or quality measures and monitoring of the dredging process. If possible, it should be avoided in the design to have comparable segment lengths as the covariant lengths. However, the segment length is not only dependent on the shear force in the shear key only. If both lengths are comparable, the design should anticipate for higher shear forces. Estimation of a covariance length can be based on site investigations and CPTs, DeGroot and Baecher (1993) presents a method for this. The thickness of the foundation material is based on the dredging tolerance. One could think of extending the quality measures or the dredging method to improve the dredging accuracy, because it would lead to a more constant thickness and stiffness and therefor a lower variability on the stiffness of the foundation layer. However in daily practice, the selection of the dredging method is depending on marine conditions and geology. The dredging method is also dictating the dredging tolerance. As an extra option, by changing the thickness of the foundation layer, the influence of the subsoil stiffness on the bedding stiffness can be decreased.

In case covariance lengths are unknown, exceedance probabilities can be found for the shear forces using NPBN and VC. There is an small

difference between NPBN and VC, where the VC is more appropriate in case of tail dependencies as in this situation. Using these methods, also conditional probabilities can be derived to simulate different possible scenarios.

In this research, only covariance lengths for the soil stiffness and dredging depth are considered and both lengths are considered as independent parameters. The latter could be topic of discussion, if the top part of the soil influences the dredging process, a correlation between both could appear. However, if the soil consist out of a multi-layer profile, this influence of the top layer on the total stiffness of the soil will reduce. In order to use this method in the design process for tunnels and even parts of the method can be used. The GRF model can be used to derive bedding stiffness to adopt in longitudinal analyses and transverse analyses. When the subsoil stiffness and the thickness of the foundation layer are inputted including their covariance lengths, or the most conservative covariance lengths (close to the segment dimensions), distributions of average bedding stiffness per segment can be derived. Using the 5% and 95% of these distributions as design values for the stiffness for an alternating bedding approach. More advanced would be the derivement of the maximum shear force using the full method. When the covariance lengths are unknown or only a know as a bandwidth, the probabilistic methods will be valuable. As conditioning can decrease the variation on the shear forces.

In reality, the soil will vary also over the support area of the tunnel. The application of the method needs adjustment, where the applicable distribution of the soil parameters develop over the area. Usually different CPTS are taken over the area. Different stiffness subsoil characterisations can be found over the support area. It is up to the designer how to account for these difference as the characterisation of the subsoil stiffness can be assumed continuous or with discrete transitions. Both options can be served using the quantile transformation to the quantiles of the local subsoil distribution.

In this method demonstration, the shear force is transferred over 2 keys. In this way, the distribution of the shear key force is statically defined. However, tunnel can be supplied with more shear keys, if needed. To account for a distribution, a design can assume that the tunnel segment will remain undeformed and that the shear forces will linearly distribute between 2 segments. If the support conditions on the segments are assumed as springs, a contribution from the segment to the shear keys can be derived. Subtracting the forces from two segments will lead to the individual shear forces for each shear key. A general assumption here is that the segments will behave independently. This assumption is valid as long as the segments will behave similarly, if the stiffness between bedding differs substantially between segments as for example at faults or at the transition to cut & cover sections this cannot be assumed.

As a recommendation for further research, more parameters should be part of the scope. Additional, the parameters used in this study are all based on a distribution with a fixed set of parameters. This could represent a single situation, however to draw more robust conclusions it is recommended to extend further research with, but not limited to:

- Multiple layers of subsoil
- Settlements
- Dredging scenarios or methods
- Non uniform loading
- Variation of IMT geometry
- Different segment lengths over the tunnel length
- More than 2 keys in the segment joint
- Interaction between 2 elements

Summarising, in order to apply the method in design, if no covariance is known, the split value (the covariance length where maximum shear key forces are to be found) for can be found based on the distributions for the various parameters found for soil stiffness and for dredging parameters. Conditioning on covariant lengths close to the split value, will result in a probability distribution for the maximum shear force. A design can be optimised in terms of reduction of the number of joints. If field research results in a covariance length of the subsoil stiffness or the dredging process is supplied with quality measures, a better understanding of the shear key force can be obtained than by application of the alternating bedding approach. An extension of this research, such as non uniform loading and more than 2 keys, will be very beneficial to the current design practice. In general, the variation of the bedding support will be based on real site variation of CPTs and an upperbound of the shear force can be found by using a conservative L_{cov} for different parameters instead of a single parameter in an alternating bedding scenario. In the hypothetical presentation of this research, the load is considered uniform as well as the subsoil stiffness characterisation. Both situations can be served using this method already and can be used in current design practice. However, when interaction between segments will occur, in case there is a significant stiffness between segments, a more sophisticated approach will be needed. The variability of the subsoil stiffness and foundation layer is still applicable, but the structural interaction behaviour should be accounted for. This analysis approach should be the ambition on short term, however there will always a balance between computer capacity in terms and more advanced analyses including several scenarios.

CRediT authorship contribution statement

Cornelis Marcel Pieter 't Hart: Conceptualization, Methodology, Software, Formal analysis, Visualization, Writing – original draft. **Oswaldo Morales-Nápoles:** Methodology, Writing – review & editing. **Bas Jonkman:** Supervision, Writing – review & editing.

Declaration of competing interest

The authors declare that they have no known competing financial interests or personal relationships that could have appeared to influence the work reported in this paper.

Data availability

No data was used for the research described in the article.

Acknowledgements

This research was supported by the Submerged Floating Tunnel (SFT) Team. This research project is commissioned by the Chinese engineering and construction company China Communications Construction Co., Ltd. (CCCC) and is jointly carried out by 8 institutions of universities, scientific research institutes, engineering consulting firms, design and construction companies. Secondly, this research was also supported by the centre for underground structures in the Netherlands (COB). As a last point, the authors would like to thank Hans de Wit and Piet Barten of TEC for their fruitful discussions and input for this research.

Appendix A. Densities for different segment lengths

See Figs. A.1–A.6.

Appendix B. Non parametric Bayesian network

B.1. Part 1: Network setup

See Figs. B.1–B.3 and Tables B.1 and B.2.

B.2. Part 1: Conditioning

See Figs. B.4–B.8 and Table B.3.

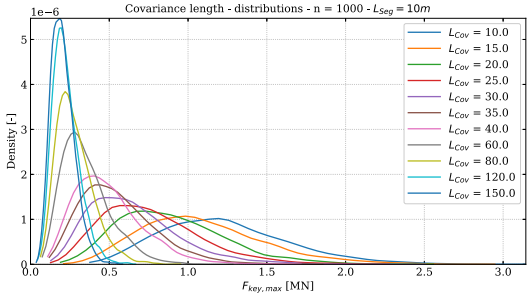

(a) Densities

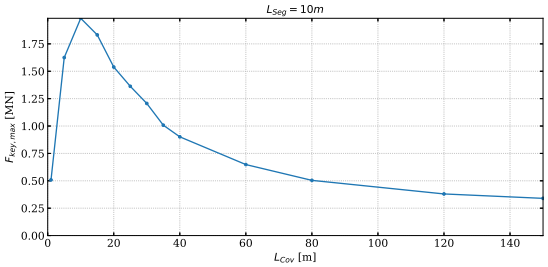

(b) Force at 95 percentile

Fig. A.1. Densities for segment length L_{seg} = 10 m.

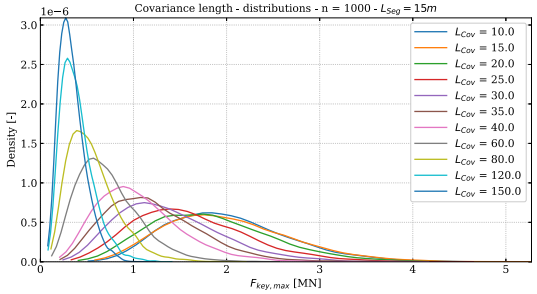

(a) Densities

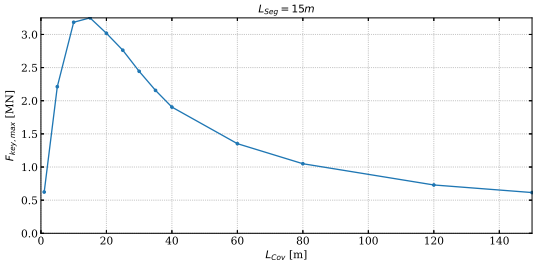

(b) Force at 95 percentile

Fig. A.2. Densities for segment length L_{seg} = 15 m.

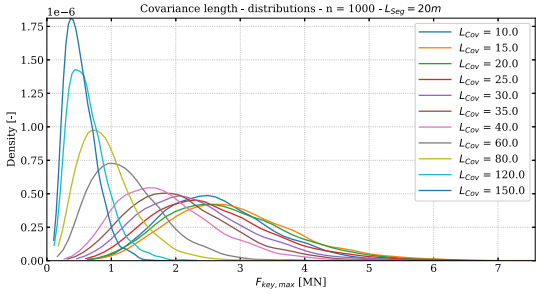

(a) Densities

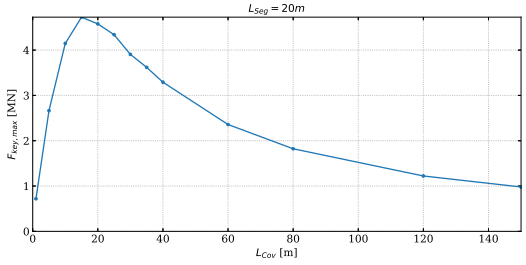

(b) Force at 95 percentile

Fig. A.3. Densities for segment length L_{seg} = 20 m.

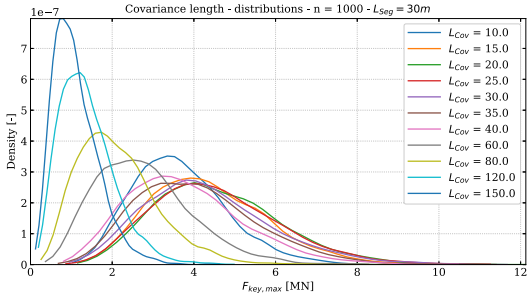

(a) Densities

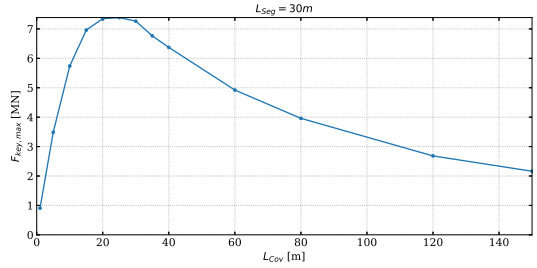

(b) Force at 95 percentile

Fig. A.4. Densities for segment length L_{seg} = 30 m.

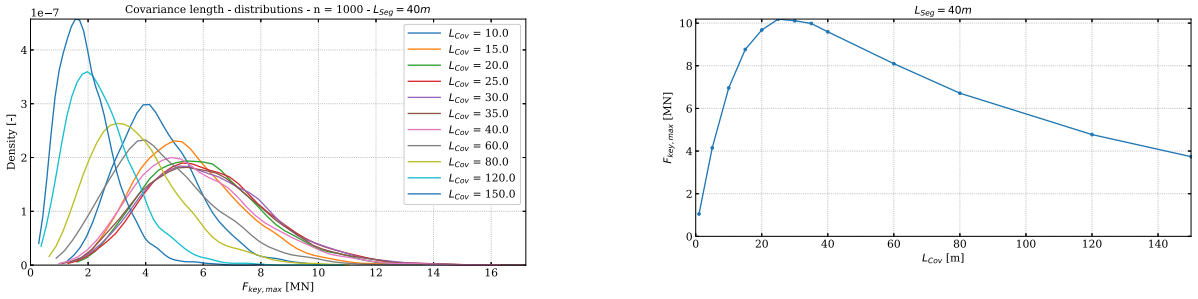

(a) Densities (b) Force at 95 percentile

Fig. A.5. Densities for segment length L_{seg} = 40 m.

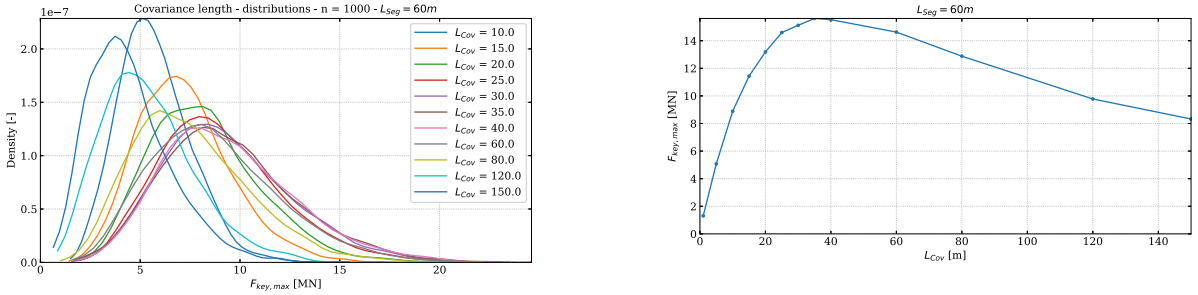

(a) Densities (b) Force at 95 percentile

Fig. A.6. Densities for segment length L_{seg} = 60 m.

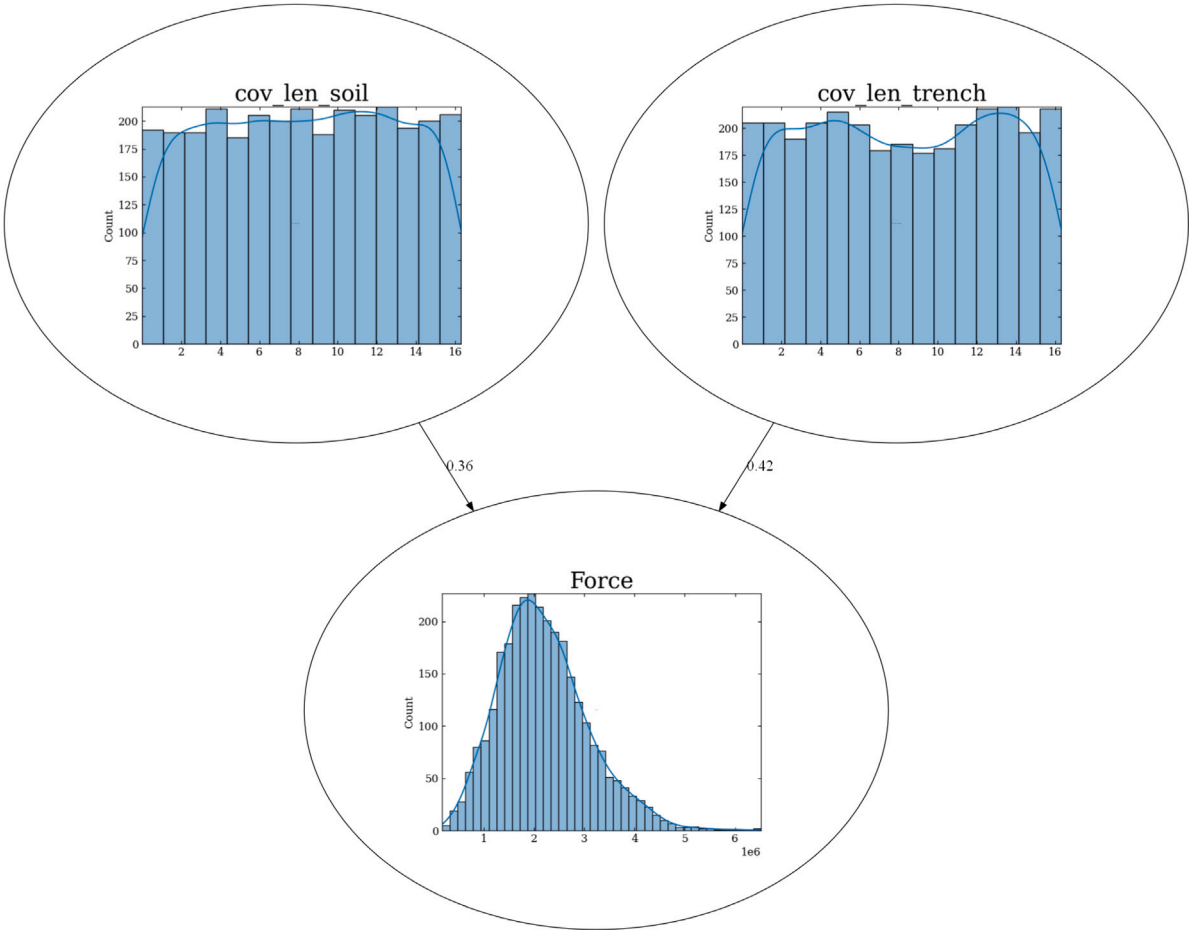

Fig. B.1. Bayesian network - part 1.

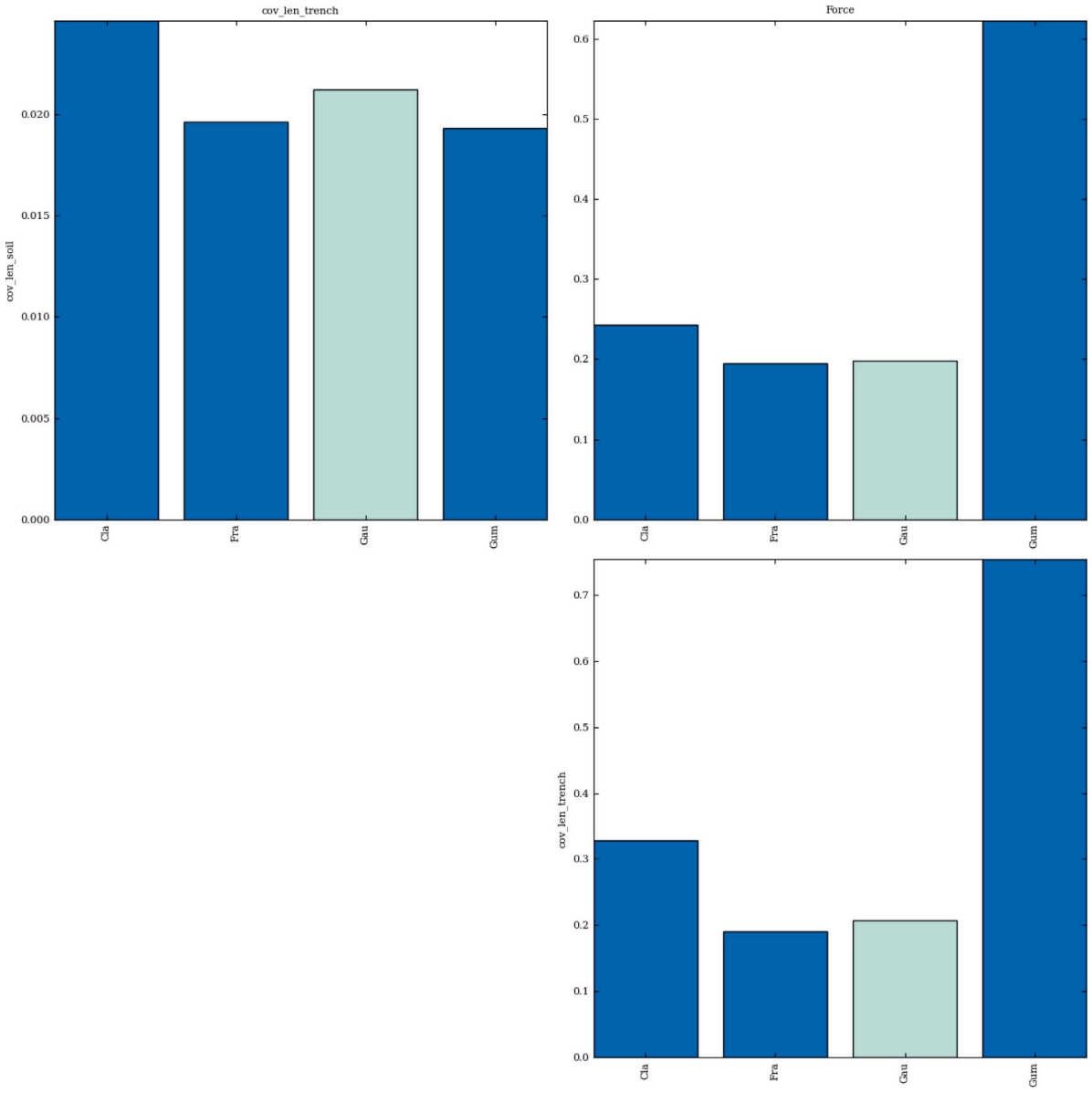

Fig. B.2. Cramer von Mises statistics - part 1.

Table B.1
Empirical rank correlation matrix for part 1.

	$L_{cov,soil}$	$L_{cov,trench}$	F_{key}
$L_{cov,soil}$	1	0.006	0.355
$L_{cov,trench}$	0.006	1	0.426
F_{key}	0.355	0.426	1

Table B.2
Conditional normal rank correlation matrix for part 1.

	$L_{cov,soil}$	$L_{cov,trench}$	F_{key}
$L_{cov,soil}$	1	0	0.355
$L_{cov,trench}$	0	1	0.424
F_{key}	0.355	0.424	1

Table B.3
Empirical rank correlation matrix for part 2.

	$L_{cov,soil}$	$L_{cov,trench}$	F_{key}
$L_{cov,soil}$	1	−0.015	−0.230
$L_{cov,trench}$	−0.015	1	−0.303
F_{key}	−0.230	−0.303	1

Table B.4
Conditional normal rank correlation matrix for part 2.

	$L_{cov,soil}$	$L_{cov,trench}$	F_{key}
$L_{cov,soil}$	1	0	−0.230
$L_{cov,trench}$	0	1	−0.307
F_{key}	−0.230	−0.307	1

B.3. Part 2: Network setup

See Figs. B.9–B.11 and Table B.4.

B.4. Part 2: Conditioning

See Figs. B.12–B.16.

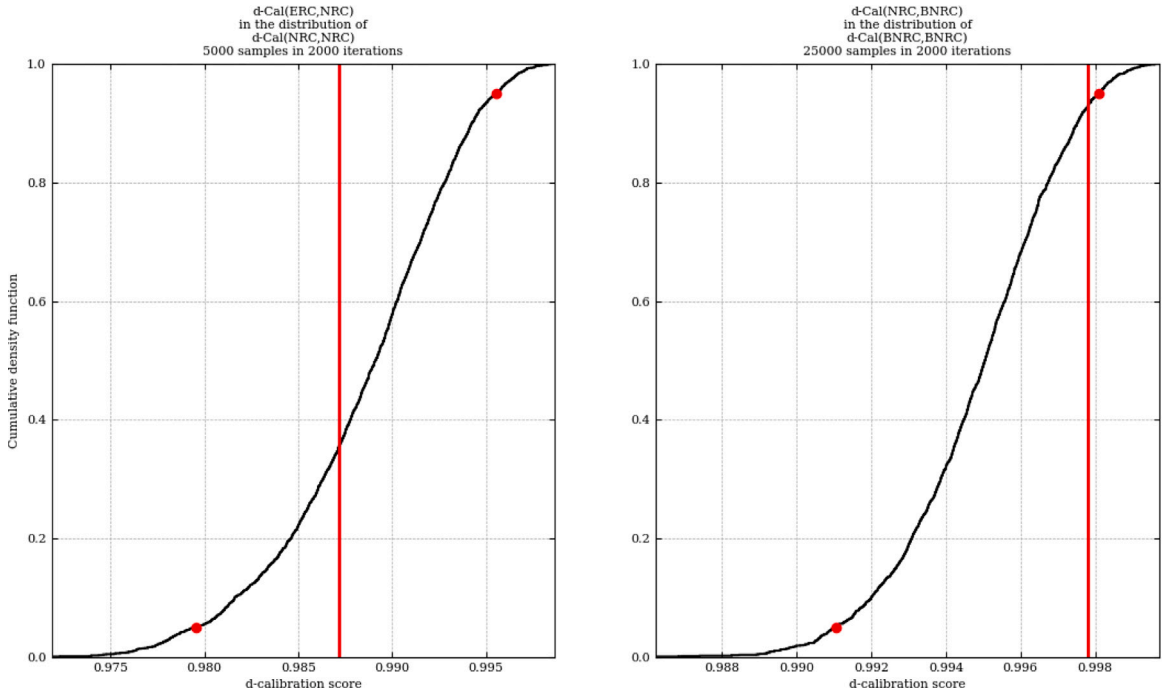

Fig. B.3. Gaussian distance (d-score) - part 1.

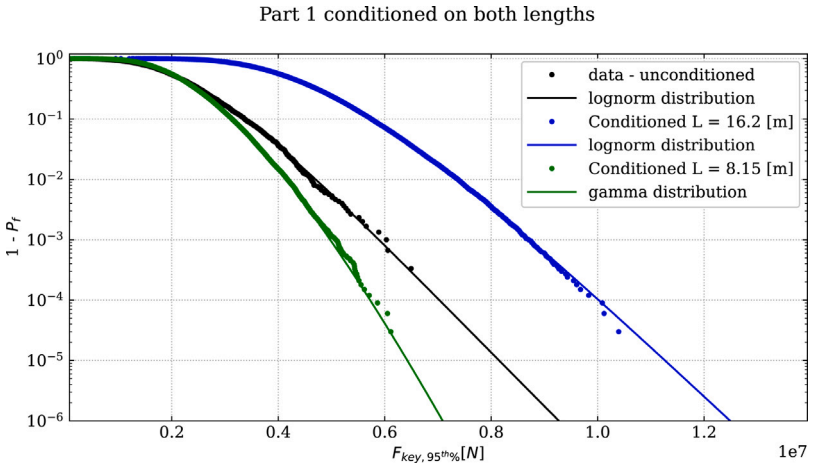

Fig. B.4. Conditioned on 2 lengths.

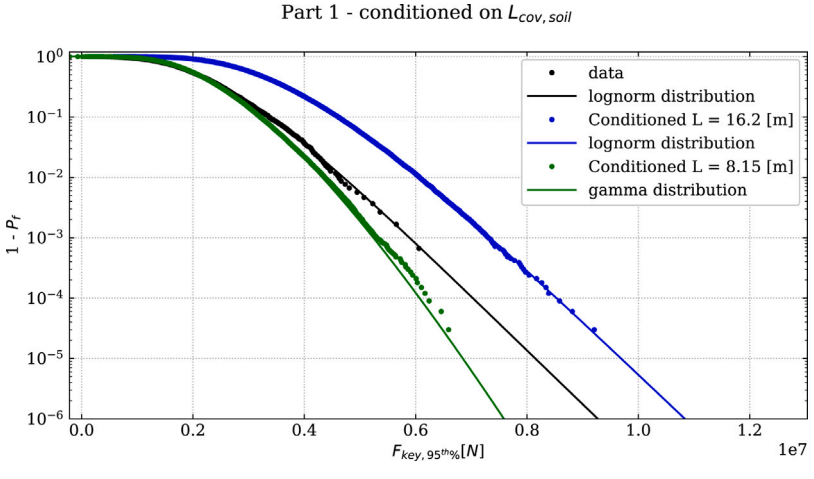

Fig. B.5. Conditioned on $L_{cov,soil}$.

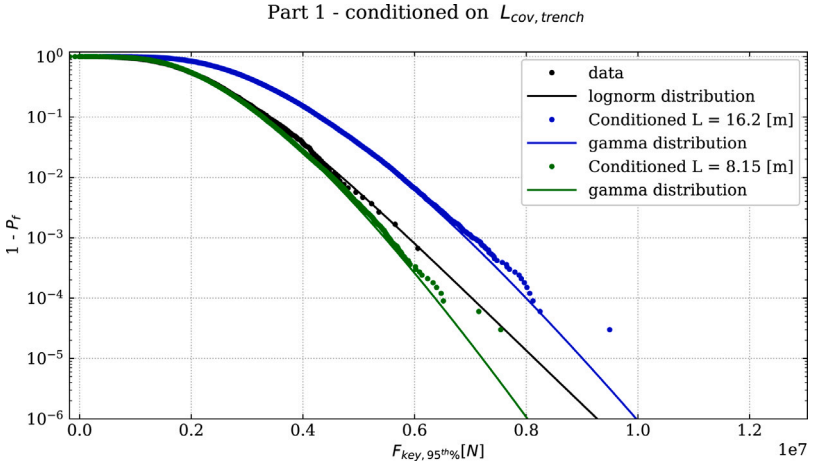

Fig. B.6. Conditioned on $L_{cov,trench}$.

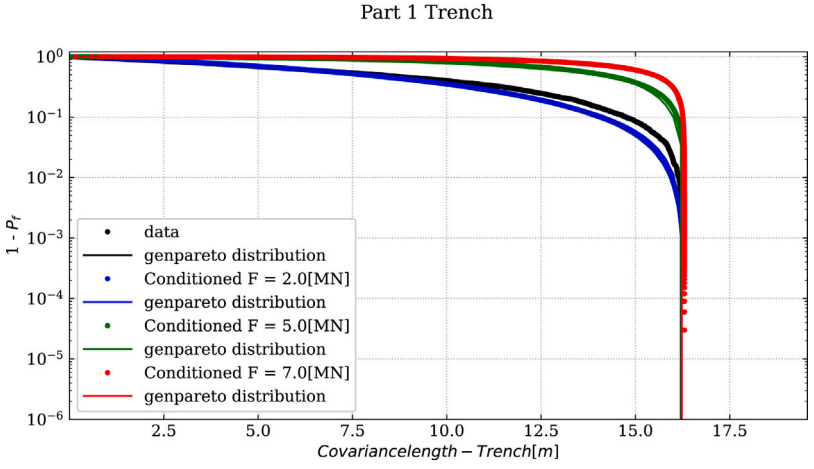

Fig. B.7. Covariance length Trench, Conditioned on Force.

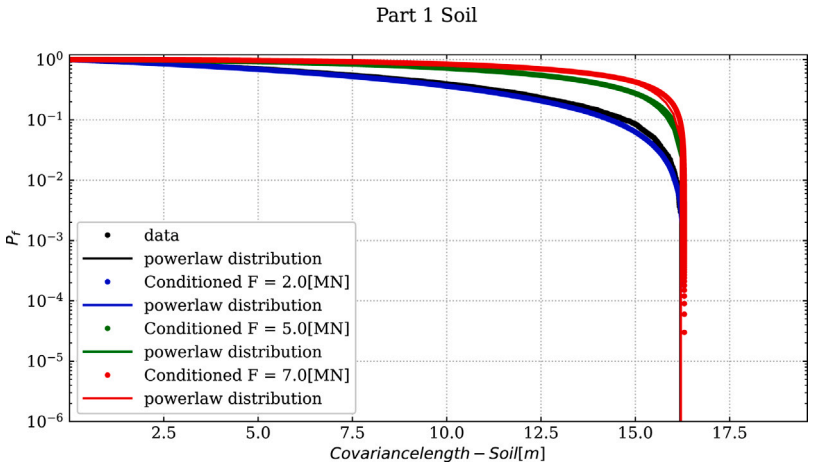

Fig. B.8. Covariance length Soil, Conditioned on Force.

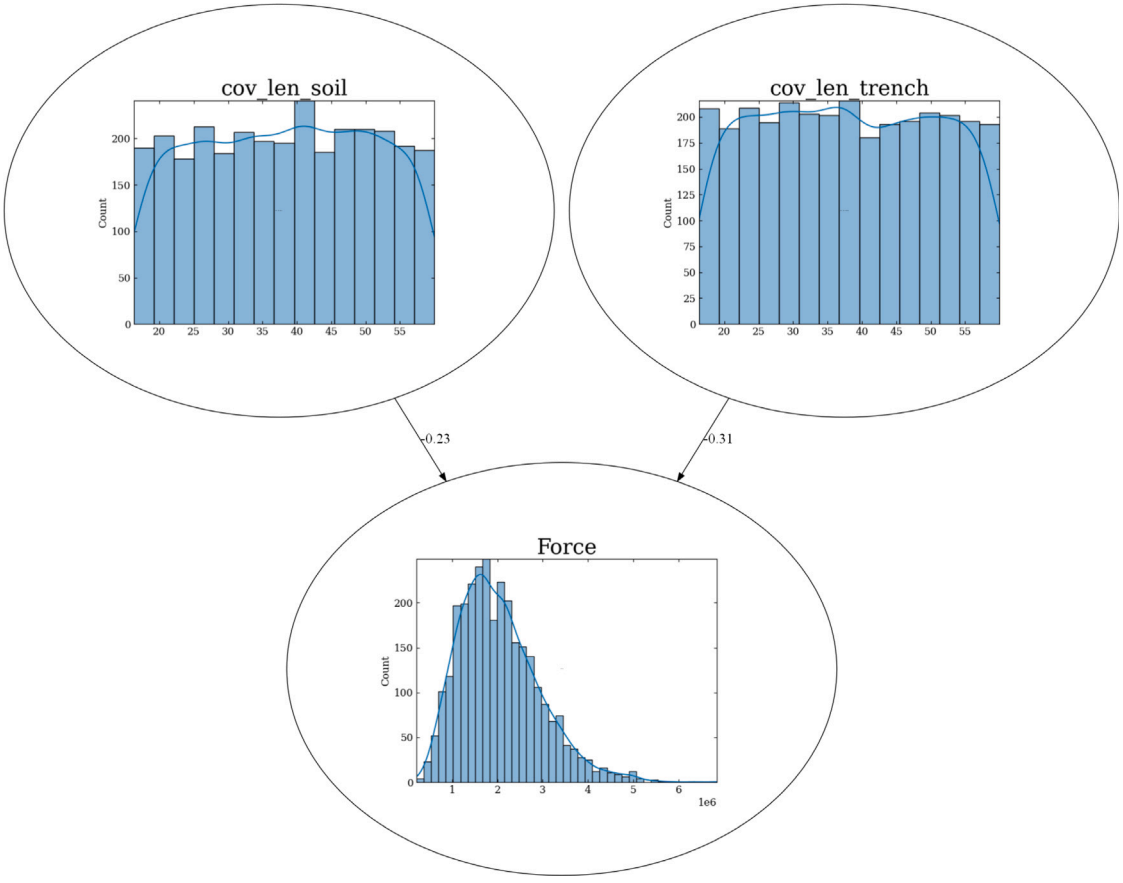

Fig. B.9. Bayesian network - part 2.

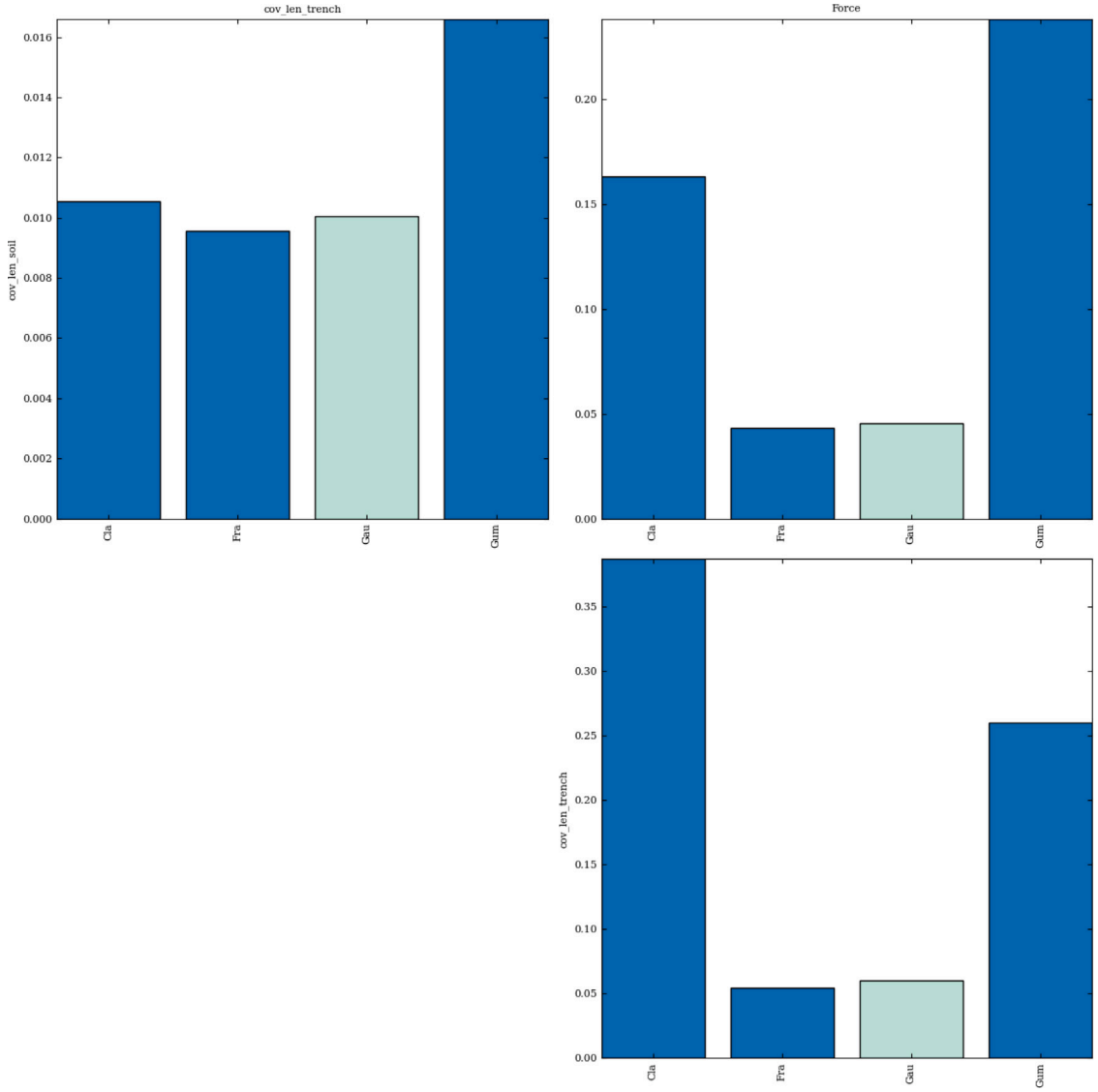

Fig. B.10. Cramer von Mises statistics - part 2.

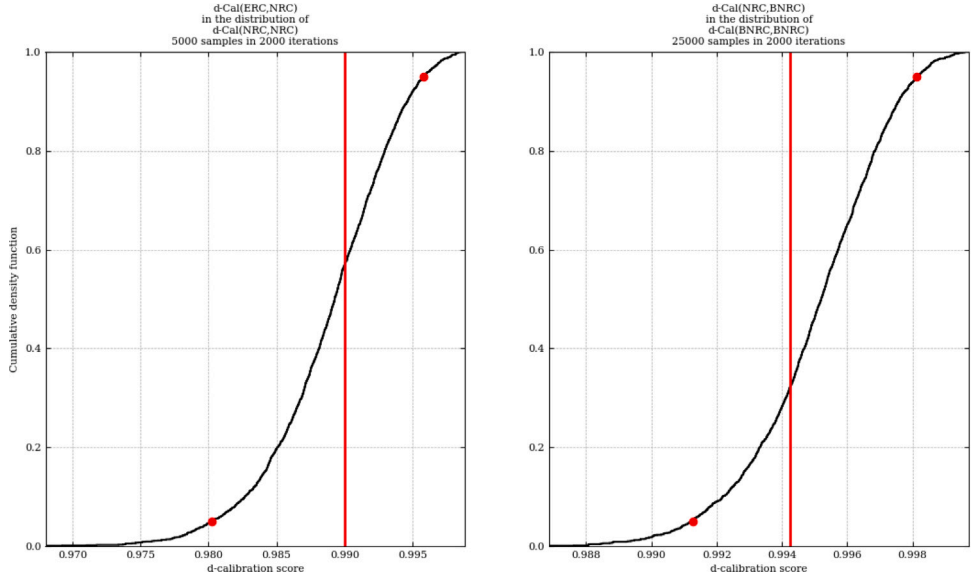

Fig. B.11. Gaussian distance (d-score) - part 2.

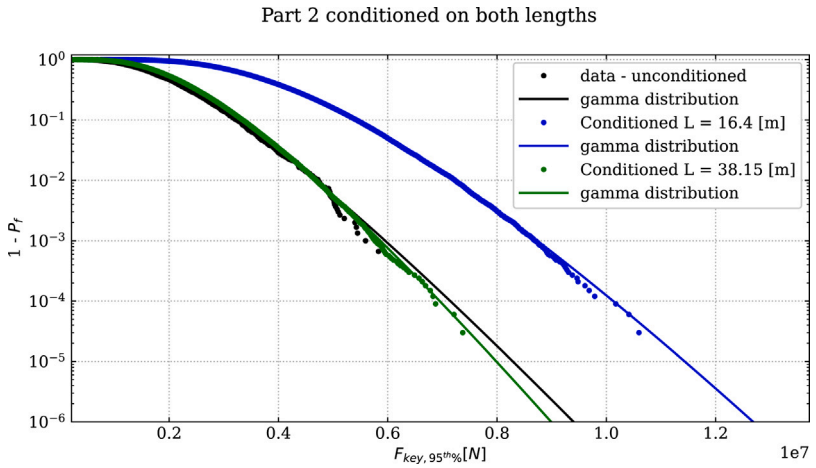

Fig. B.12. Conditioned on 2 lengths.

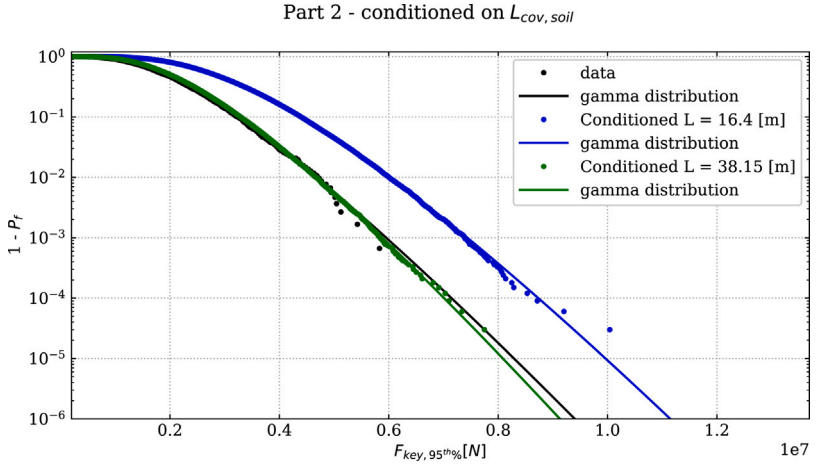

Fig. B.13. Conditioned on $L_{cov,soil}$.

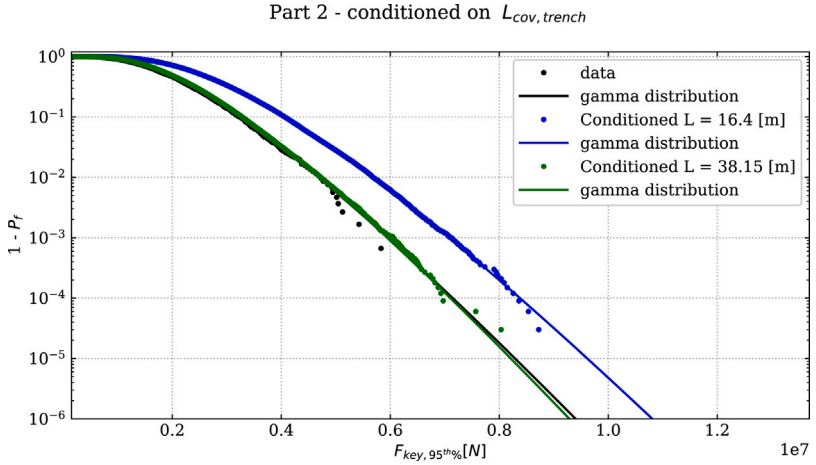

Fig. B.14. Conditioned on $L_{cov,trench}$.

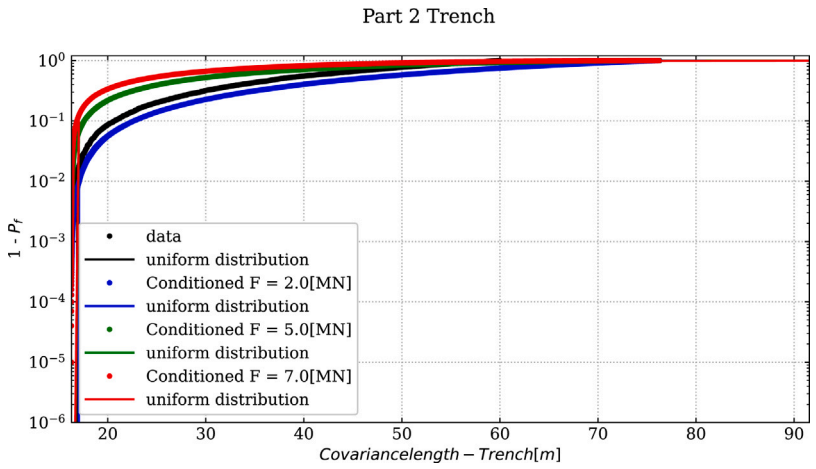

Fig. B.15. Covariance length Trench, Conditioned on Force.

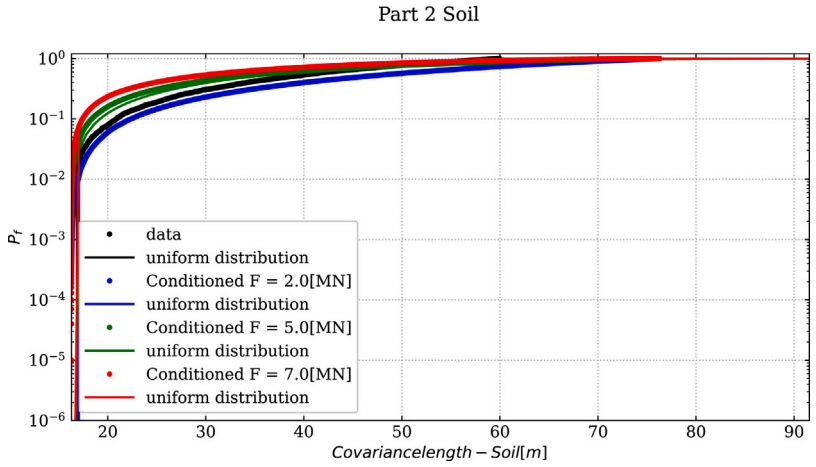

Fig. B.16. Covariance length Soil, Conditioned on Force.

Table C.1
Correlation matrix Part 1.

	$L_{cov;soil}$	$L_{cov;trench}$	Shear force
$L_{cov;soil}$	1.0	0.01	0.36
$L_{cov;trench}$	0.01	1.0	0.44
Shear Force	0.36	0.44	1.0

Appendix C. Vine copulas

C.1. Part 1: Data

See Tables C.1 and C.2.

C.1.1. Matrix based on 3-1-2 - part 1

$$M = \begin{bmatrix} 1 & 1 & 1 \\ 2 & 2 & 0 \\ 3 & 0 & 0 \end{bmatrix}$$

Trees - Trace
$** Tree : 0$
$3,1 <-> Gaussian, parameters = 0.371329$
$2,1 <-> Joe, parameters = 1.00767$
$** Tree : 1$
$3,2|1 <-> Gumbel180°, parameters = 1.46212$
AIC score: -1260.5

C.1.2. Matrix based on 2-3-1 - part 1

$$M = \begin{bmatrix} 3 & 3 & 3 \\ 1 & 1 & 0 \\ 2 & 0 & 0 \end{bmatrix}$$

Trees - Trace
$** Tree : 0$
$2,3 <-> Gumbel180°, parameters = 1.38855$
$1,3 <-> Gaussian, parameters = 0.371329$
$** Tree : 1$
$2,1|3 <-> Frank, parameters = -1.4251$
AIC score: -1255.2

C.1.3. Matrix based on 1-2-3 - part 1

$$M = \begin{bmatrix} 2 & 2 & 2 \\ 3 & 3 & 0 \\ 1 & 0 & 0 \end{bmatrix}$$

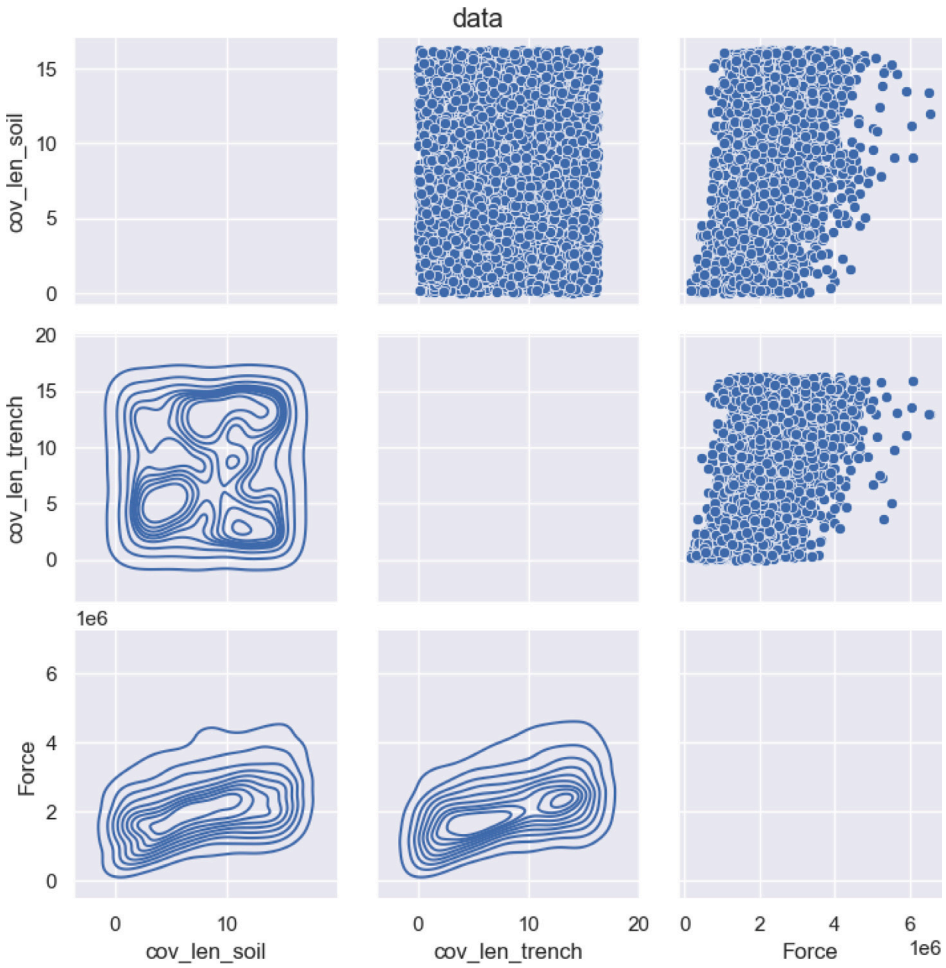

Fig. C.1. Data overview.

Table C.2
Correlation matrix Part 2.

	$L_{cov;soil}$	$L_{cov;trench}$	Shear force
$L_{cov;soil}$	1.0	–0.02	–0.24
$L_{cov;trench}$	–0.02	1.0	–0.31
Shear Force	–0.24	–0.31	1.0

Trees - Trace
$**\ Tree\ :\ 0$
$1,2 < -> Joe, parameters = 1.00767$
$3,2 < -> Gumbel180°, parameters = 1.38855$
$**\ Tree\ :\ 1$
$1,3|2 < -> Frank, parameters = 2.79775$
AIC score: -1254.9

C.2. Part 1: Conditioning - vines

C.3. Part 2: Data

C.3.1. Matrix based on 3-1-2 - part 2

$$M = \begin{bmatrix} 1 & 1 & 1 \\ 2 & 2 & 0 \\ 3 & 0 & 0 \end{bmatrix}$$

Trees - Trace $** Tree\ :\ 0\ 3,1 < -> Frank, parameters = -1.48861$ $2,1 < -> Frank, parameters = -0.1289$ $** Tree\ :\ 1\ 3,2|1 < -> Gaussian, parameters = -0.331021$
AIC score: -520.3

C.3.2. Matrix based on 2-3-1 - part 2

$$M = \begin{bmatrix} 3 & 3 & 3 \\ 1 & 1 & 0 \\ 2 & 0 & 0 \end{bmatrix}$$

Trees - Trace
$** Tree\ :\ 0\ 2,3 < -> Frank, parameters = -1.99834\ 1,3 < -> Frank, parameters = -1.48861 ** Tree\ :\ 1\ 2,1|3 < -> Frank, parameters = -0.614899$
AIC score: -521.4 (see Fig. C.1).

C.3.3. Matrix based on 1-2-3 - part 2

$$M = \begin{bmatrix} 2 & 2 & 2 \\ 3 & 3 & 0 \\ 1 & 0 & 0 \end{bmatrix}$$

Trees - Trace $** Tree\ :\ 0\ 1,2 < -> Frank, parameters = -0.1289$ $3,2 < -> Frank, parameters = -1.99834 ** Tree\ :\ 1\ 1,3|2 < -> Gaussian, parameters = -0.260272$
AIC score: -519.9 (see Figs. C.3–C.9).

C.4. Part 2: Conditioning - Vines

See Figs. C.10–C.16.

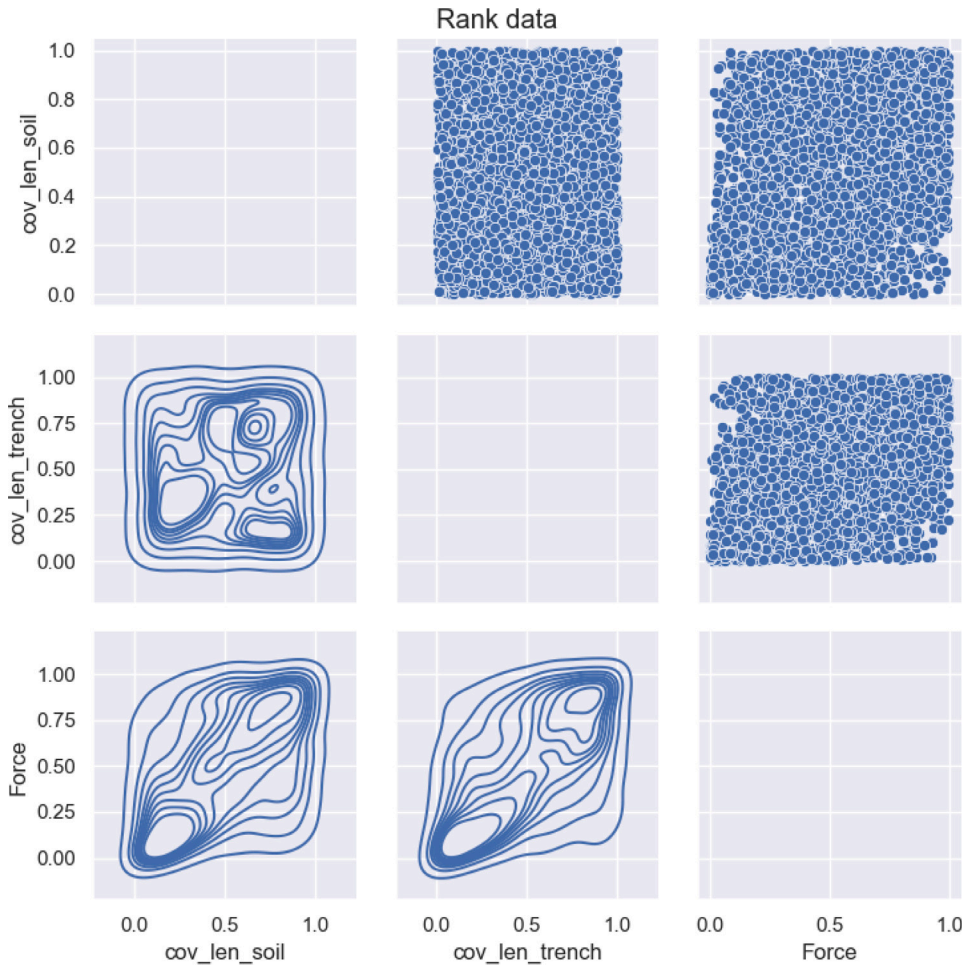

Fig. C.2. Data overview - in [0,1].

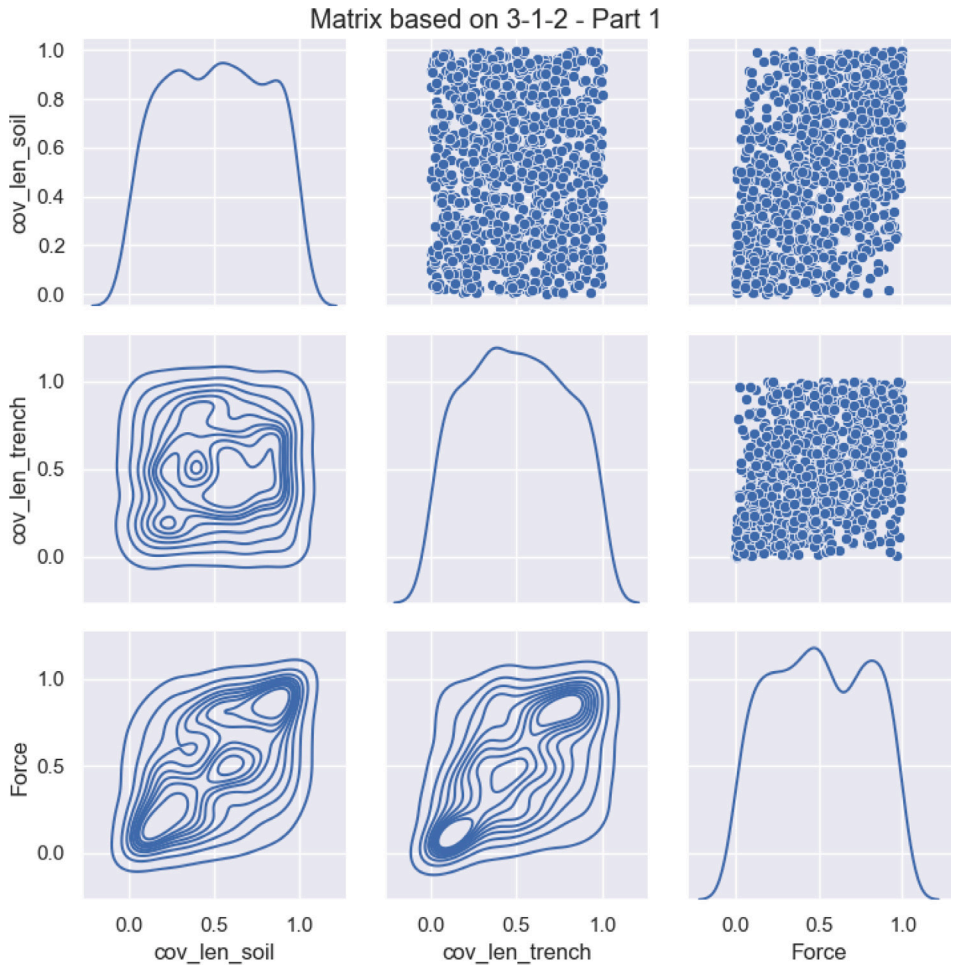

Fig. C.3. Sampling - matrix 3-1-2 - Part 1.

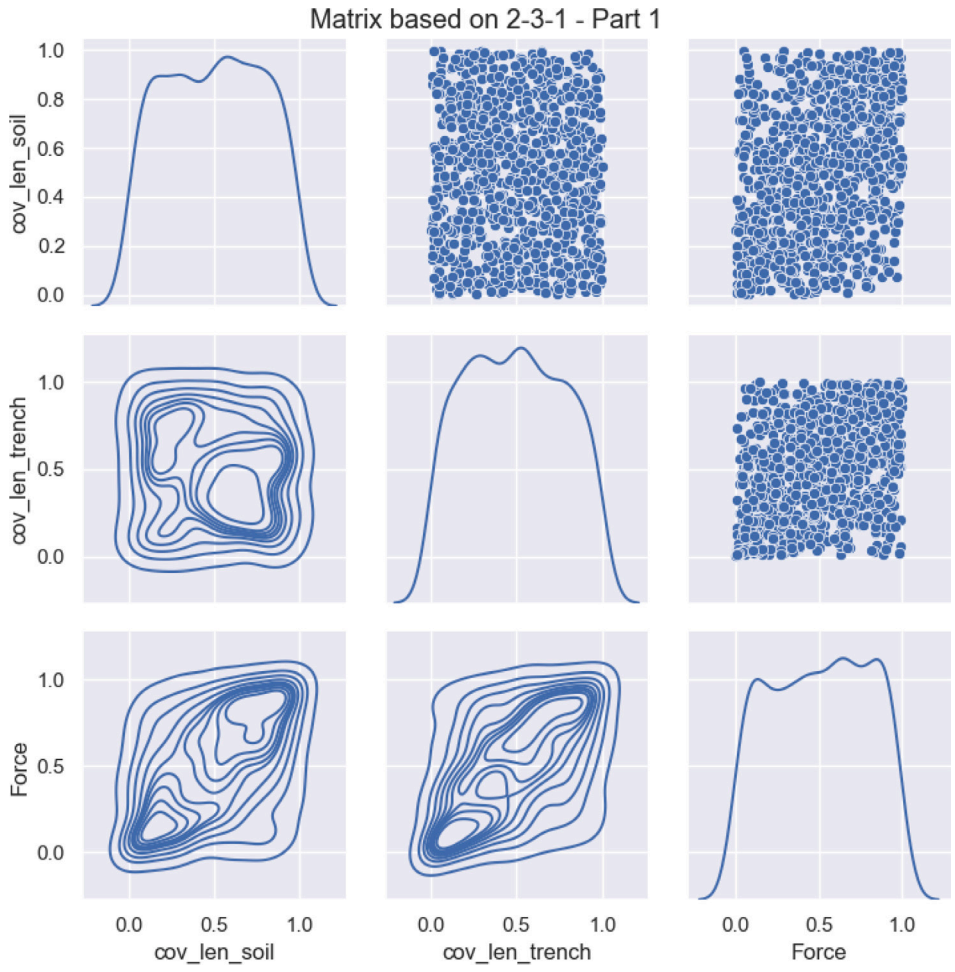

Fig. C.4. Sampling - matrix 2-3-1 - Part 1.

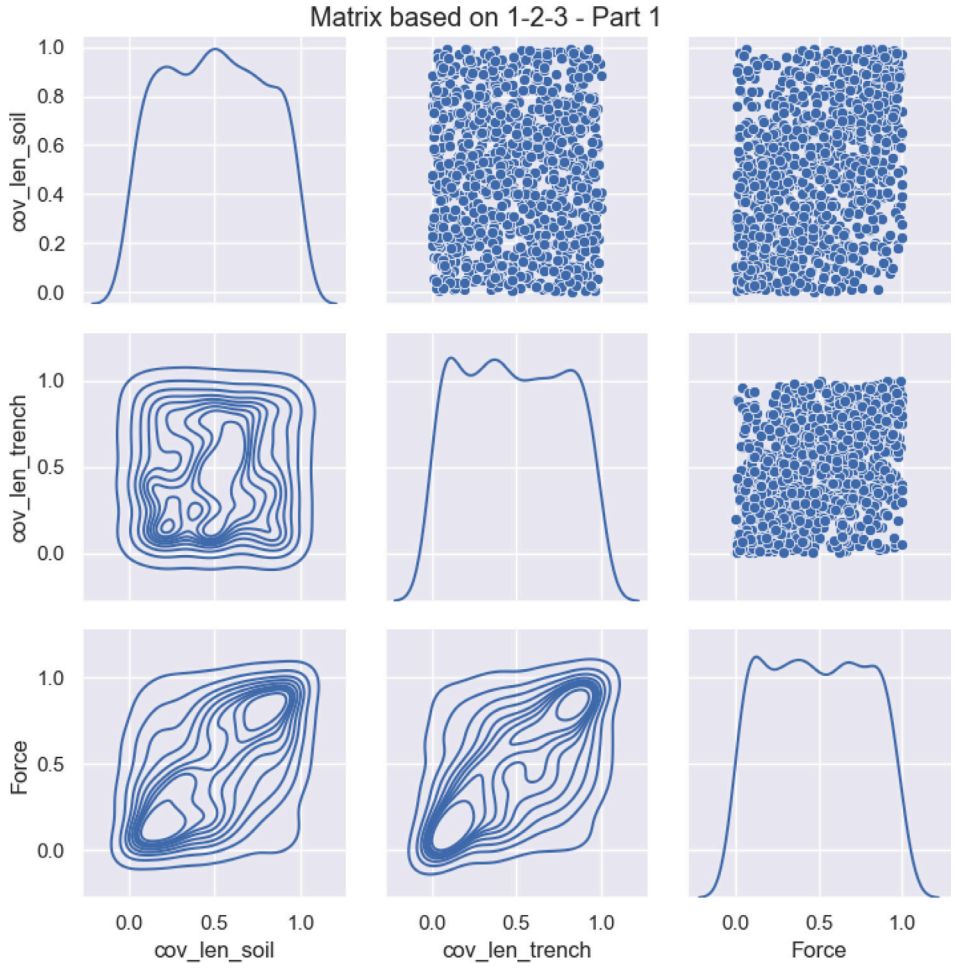

Fig. C.5. Sampling - matrix 1-2-3 - Part 1.

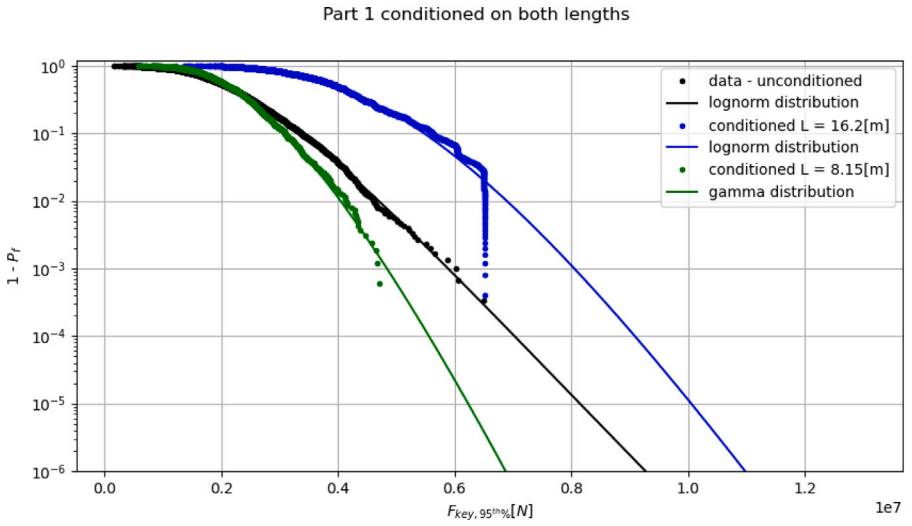

Fig. C.6. Conditioned on 2 lengths.

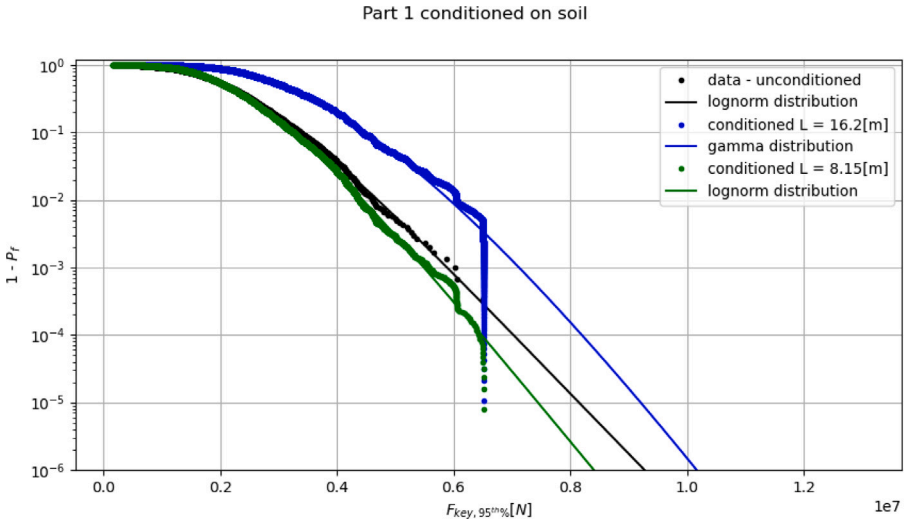

Fig. C.7. Conditioned on $L_{cov,soil}$.

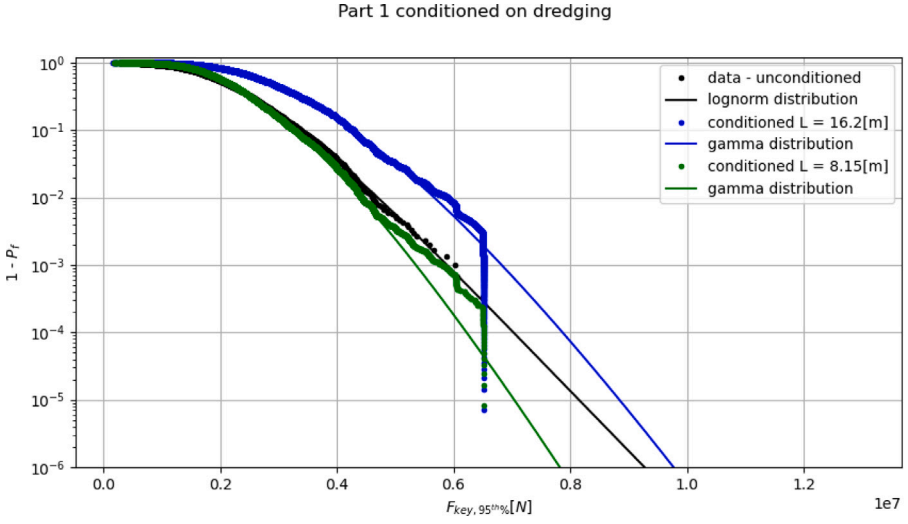

Fig. C.8. Conditioned on $L_{cov,trench}$.

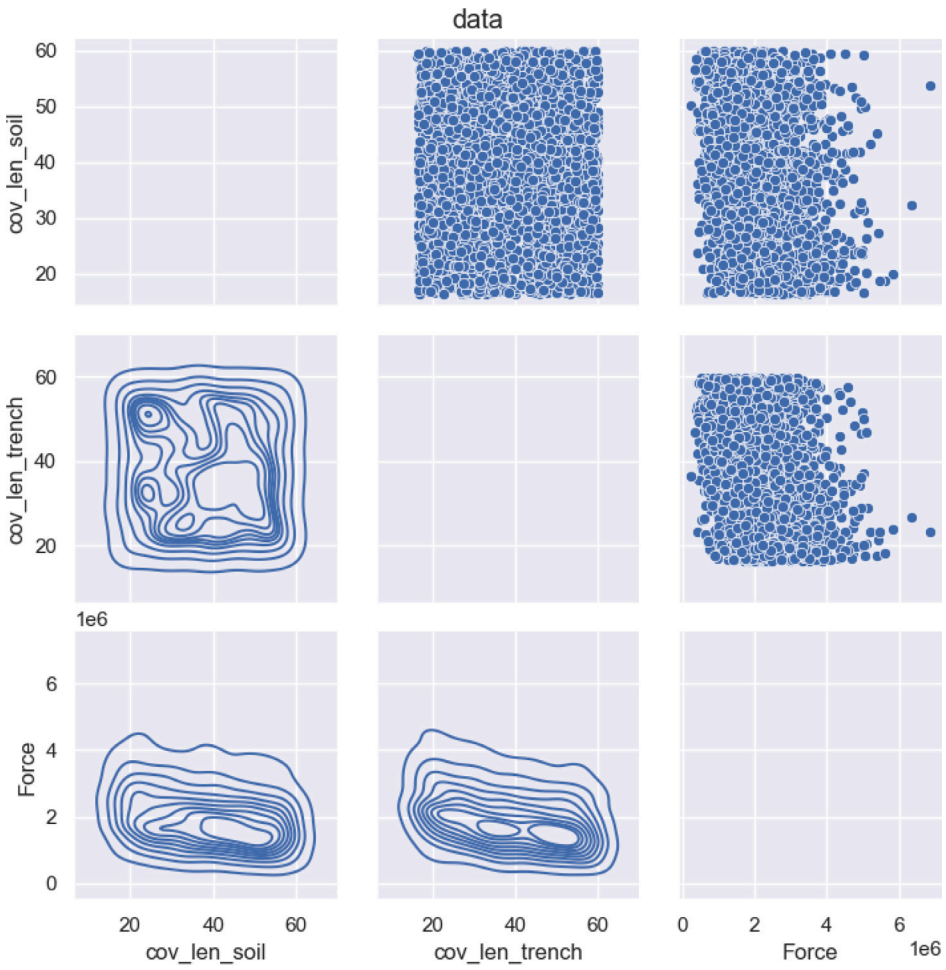

Fig. C.9. Data overview.

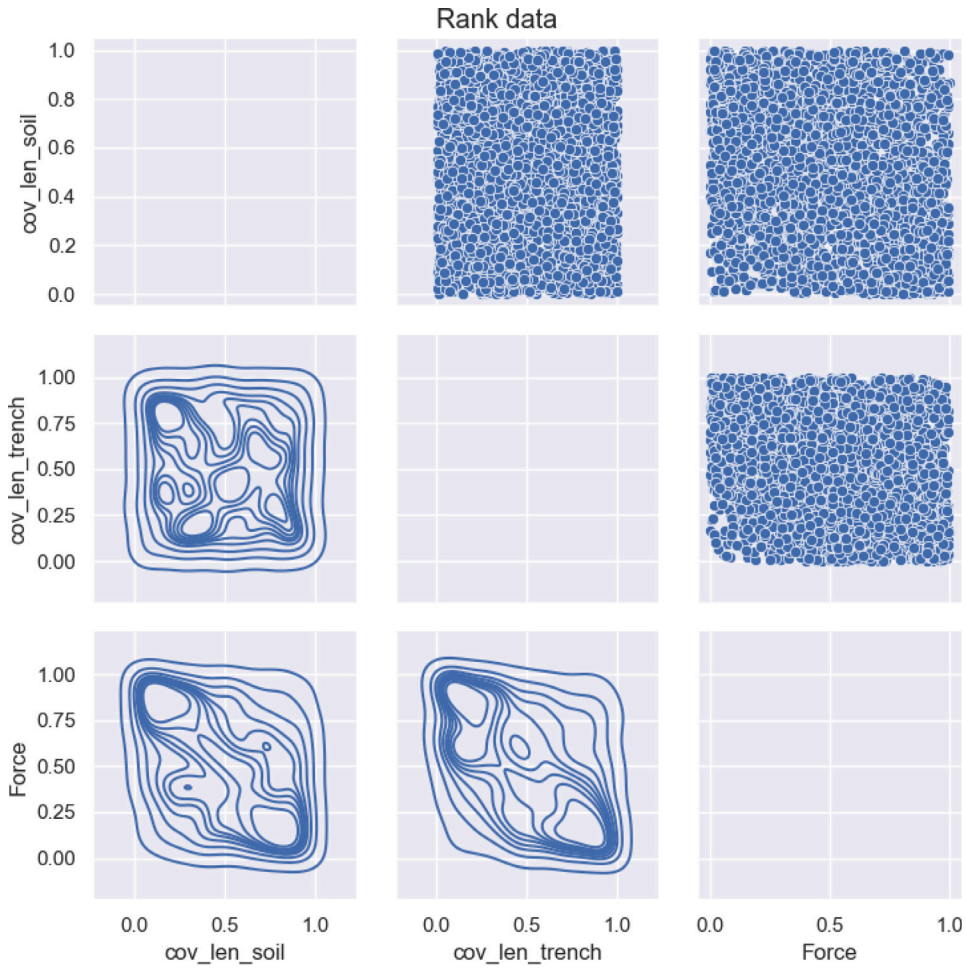

Fig. C.10. Data overview - in [0,1].

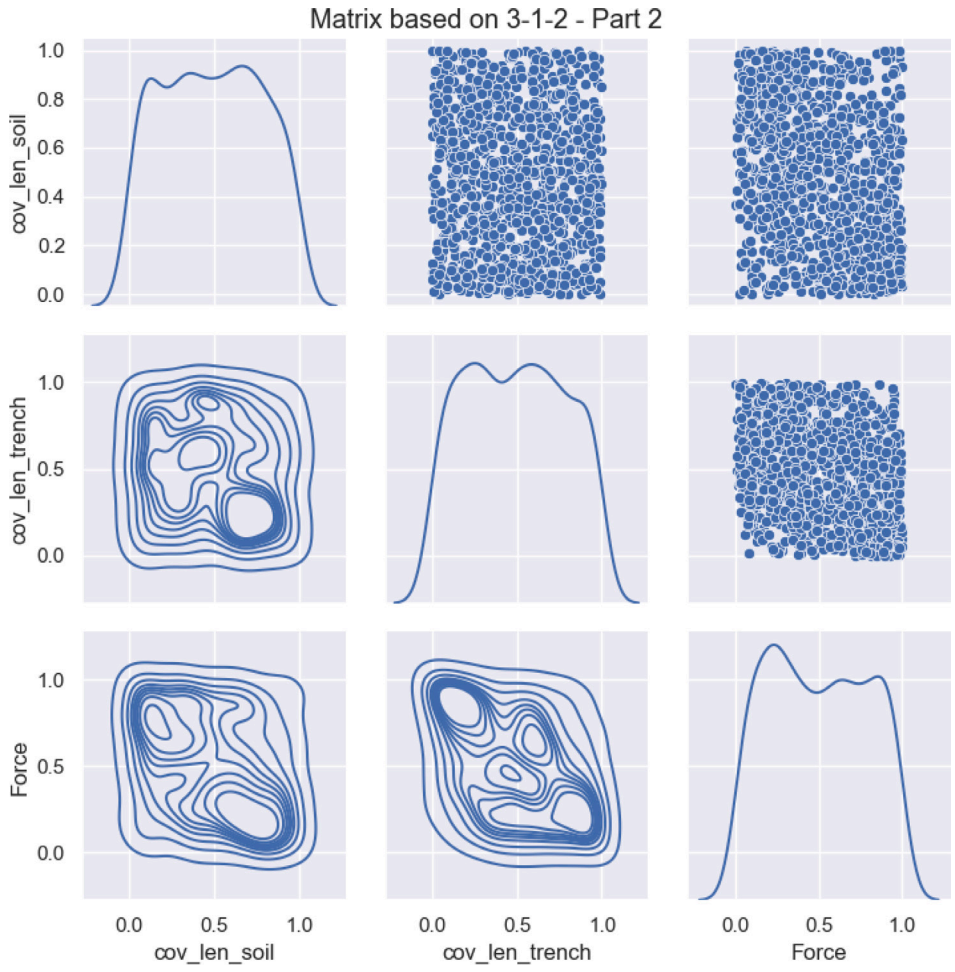

Fig. C.11. Sampling - matrix 3-1-2 - Part 2.

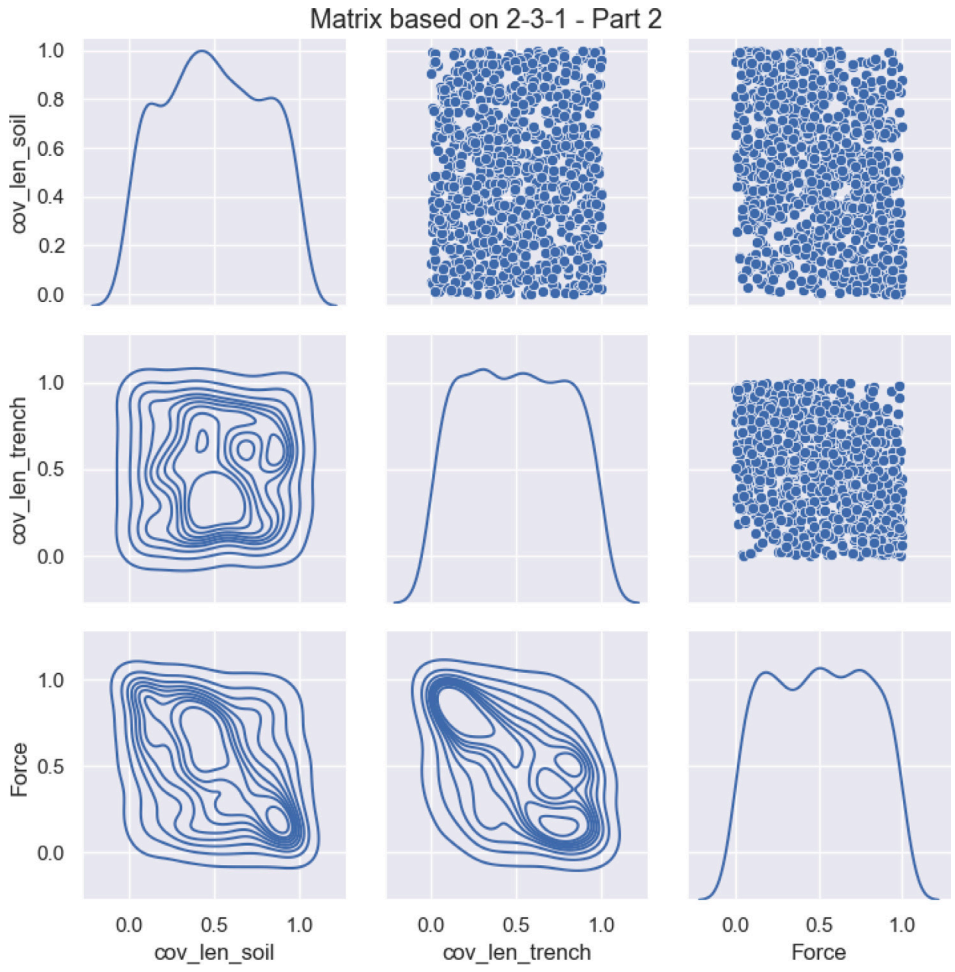

Fig. C.12. Sampling - matrix 2-3-1 - Part 2.

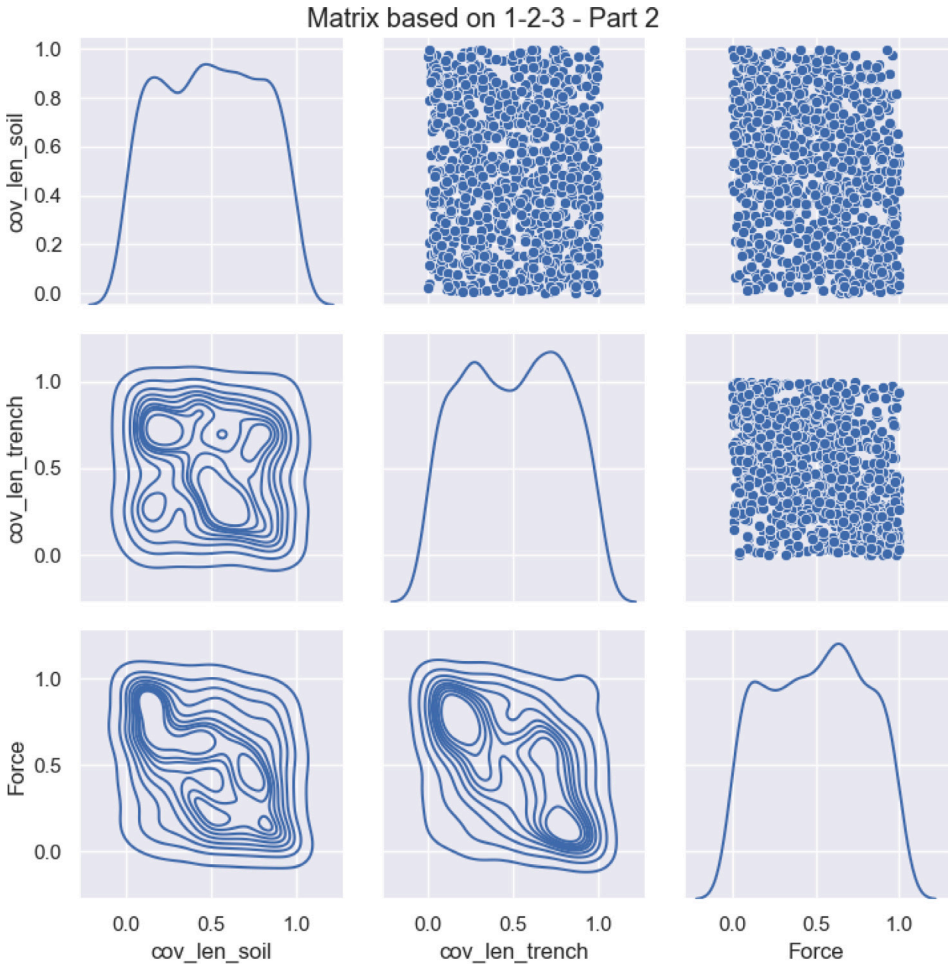

Fig. C.13. Sampling - matrix 1-2-3 - Part 2.

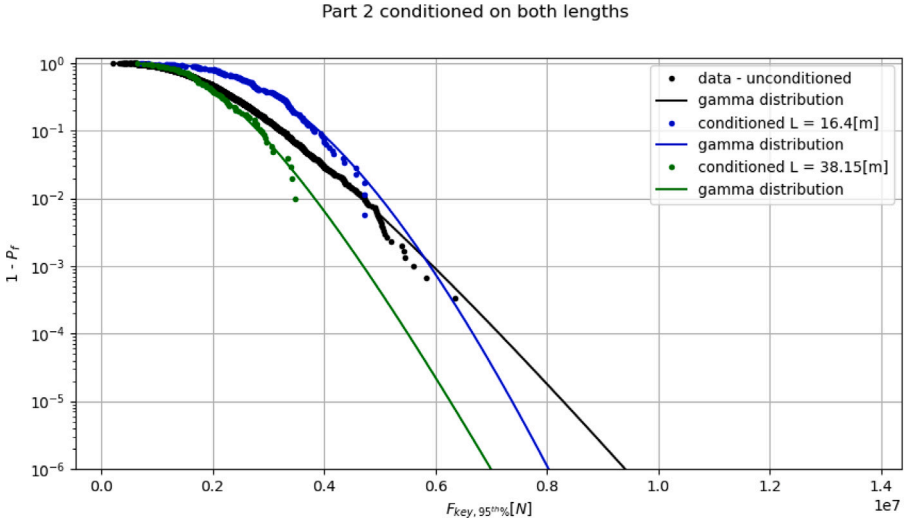

Fig. C.14. Conditioned on 2 lengths.

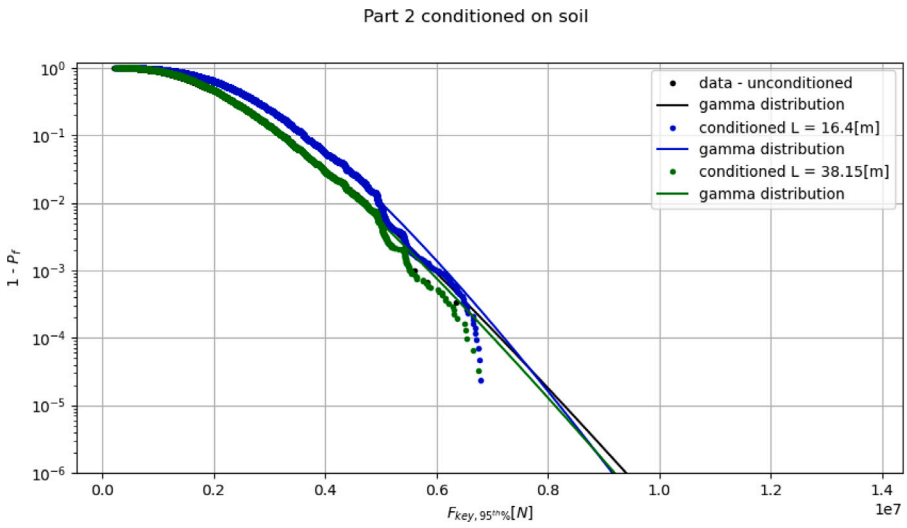

Fig. C.15. Conditioned on $L_{cov,soil}$.

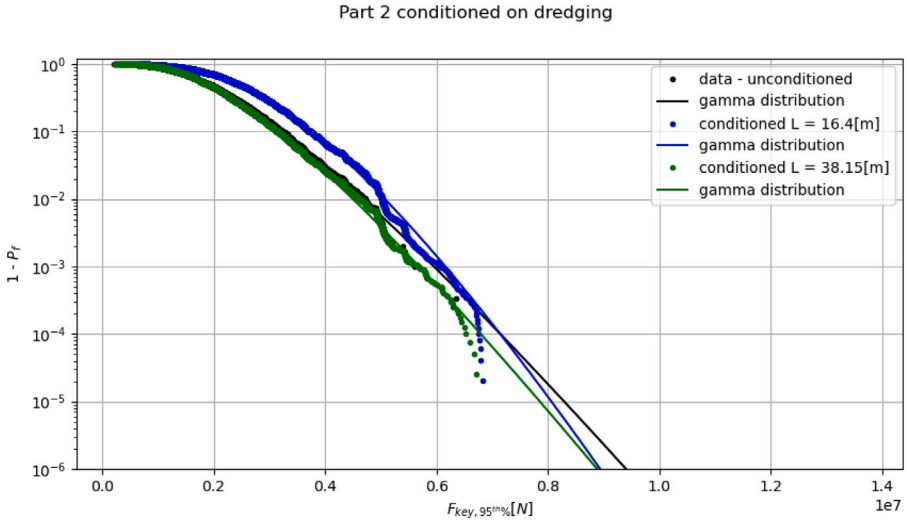

Fig. C.16. Conditioned on $L_{cov,trench}$.

References

Aas, K., Berg, D., 2009. Models for construction of multivariate dependence. Eur. J. Finance 15, 639–659. http://dx.doi.org/10.1080/13518470802588767.

Aas, K., Czado, C., Frigessi, A., Bakken, H., 2009. Pair-copula constructions of multiple dependence. Insurance Math. Econom. 44, 182–198. http://dx.doi.org/10.1016/j.insmatheco.2007.02.001.

Adler, R., Taylor, J., 2009. Random Fields and Geometry. Springer Monographs in Mathematics, Springer New York.

Bocchini, P., 2008. Probabilistic Approaches in Civil Engineering: Generation of Random Fields and Structural Identification with Genetic Algorithms (Ph.D. thesis). Università di Bologna.

Bucher, C., 2006. Applications of random field models in stochastic structural mechanics. In: Advances in Engineering Structures, Mechanics & Construction, vol. 140, pp. 471–484. http://dx.doi.org/10.1007/1-4020-4891-2_39.

Cheng, H., Chen, J., Chen, R., Chen, G., 2019. Comparison of modeling soil parameters using random variables and random fields in reliability analysis of tunnel face. Int. J. Geomech. 19, 04018184. http://dx.doi.org/10.1061/(ASCE)GM.1943-5622.0001330.

Chollete, L., Heinen, A., Valdesogo, A., 2008. Modeling international financial returns with a multivariate regime switching copula. SSRN Electron. J. 7, http://dx.doi.org/10.2139/ssrn.1102632.

Couasnon, A., Sebastian, A., Morales-Nápoles, O., 2018. A copula-based bayesian network for modeling compound flood hazard from riverine and coastal interactions at the catchment scale: An application to the houston ship channel, Texas. Water (Switzerland) 10 (9), http://dx.doi.org/10.3390/w10091190.

de Wit, J., van Putten, E., 2014. The immersed tunnel as fixed link – a successful alternative pushed by innovation. In: Proceedings of the World Tunnel Congress.

DeGroot, D., Baecher, G., 1993. Estimating autocovariance of in-situ soil properties. J. Geotech. Eng. 119, http://dx.doi.org/10.1061/(ASCE)0733-9410(1993)119:1(147).

European Committee for Standardization, 2002. EN 1990. Eurocode: Basis of structural design. CEN, Brussels.

Glerum, A., 1992. Options for tunneling: a personal story. Tunn. Undergr. Space Technol. 7 (4), 313–315. http://dx.doi.org/10.1016/0886-7798(92)90059-Q, URL: https://www.sciencedirect.com/science/article/pii/088677989290059Q.

Glerum, A., 1995. Developments in immersed tunnelling in holland. Tunn. Undergr. Space Technol. 10 (4), 455–462. http://dx.doi.org/10.1016/0886-7798(95)00031-S, URL: https://www.sciencedirect.com/science/article/pii/088677989500031S.

Gong, W., Juang, C.H., Martin, J., Tang, H., Wang, Q., Huang, H., 2018. Probabilistic analysis of tunnel longitudinal performance based upon conditional random field simulation of soil properties. Tunn. Undergr. Space Technol. 73, 1–14. http://dx.doi.org/10.1016/j.tust.2017.11.026.

Grantz, W., 1997. Chapter 3 structural design of immersed tunnels. Tunn. Undergr. Space Technol. 12, 93–109. http://dx.doi.org/10.1016/S0886-7798(97)90015-8.

Gravesen, L., Rasmussen, N.S., 1993. A milestone in tunnelling: Rotterdam's Maas tunnel celebrates its fiftieth anniversary. Tunn. Undergr. Space Technol. 8 (4), 413–424. http://dx.doi.org/10.1016/0886-7798(93)90003-E, URL: https://www.sciencedirect.com/science/article/pii/088677989390003E.

Guennebaud, G., Jacob, B., et al., 2010. Eigen v3. http://eigen.tuxfamily.org.

Hanea, A., Morales Napoles, O., Ababei, D., 2015. Non-parametric Bayesian networks: Improving theory and reviewing applications. Reliab. Eng. Syst. Saf. 144, 265–284. http://dx.doi.org/10.1016/j.ress.2015.07.027, URL: https://www.sciencedirect.com/science/article/pii/S0951832015002331.

Hicks, M.A., Li, Y., 2018. Influence of length effect on embankment slope reliability in 3D. Int. J. Numer. Anal. Methods Geomech. 42 (7), 891–915. http://dx.doi.org/10.1002/nag.2766, URL: https://onlinelibrary.wiley.com/doi/abs/10.1002/nag.2766.

Hristopulos, D.T., 2020. Random fields for spatial data modeling, a primer for scientists and engineers. http://dx.doi.org/10.1007/978-94-024-1918-4, URL: https://app.dimensions.ai/details/publication/pub.1124916302.

Jäger, W., Nápoles, O., 2017. A vine-copula model for time series of significant wave heights and mean zero-crossing periods in the north sea. ASCE-ASME J. Risk Uncertain. Eng. Syst. A 3 (4), http://dx.doi.org/10.1061/AJRUA6.0000917.

Joe, H., 2014. Dependence modeling with copulas. In: Chapman & Hall/CRC Monographs on Statistics & Applied Probability. Taylor & Francis.

Kasama, K., Zen, K., 2011. Effects of spatial variability of soil property on slope stability. In: Proceedings, First International Symposium on Uncertainty Modeling and Analysis and Management. ICVRAM 2011, pp. 691–698. http://dx.doi.org/10.1061/41170(400)84.

Koot, P., Mendoza-Lugo, M.A., Paprotny, D., Morales-Nápoles, O., Ragno, E., Worm, D.T., 2023. Pybanshee version (1.0): A python implementation of the MATLAB toolbox BANSHEE for non-parametric Bayesian networks with updated features. SoftwareX 21, 101279. http://dx.doi.org/10.1016/j.softx.2022.101279, URL: https://www.sciencedirect.com/science/article/pii/S2352711022001972.

Li, W., Fang, Y., Mo, H., Gu, R., Chen, J., Wang, Y., Feng, D., 2014. Model test of immersed tube tunnel foundation treated by sand-flow method. Tunn. Undergr. Space Technol. 40, 102–108. http://dx.doi.org/10.1016/j.tust.2013.09.015, URL: https://www.sciencedirect.com/science/article/pii/S0886779813001454.

Li, Y., Hicks, M., Vardon, P., 2017. Cost-effective design of long spatially variable soil slopes using conditional simulation. In: Geo-Risk 2017. pp. 394–402. http://dx.doi.org/10.1061/9780784480700.038.

Liu, Y., Li, J., Sun, S., Yu, B., 2019. Advances in Gaussian random field generation: a review. Comput. Geosci. 23 (5), 1011–1047.

Mendoza-Lugo, M., Delgado-Hernández, D., Morales-Nápoles, O., 2019. Reliability analysis of reinforced concrete vehicle bridges columns using non-parametric Bayesian networks. Eng. Struct. 188, 178–187. http://dx.doi.org/10.1016/j.engstruct.2019.03.011.

Mendoza-Lugo, M.A., Morales-Nápoles, O., Delgado-Hernández, D.J., 2022. A non-parametric Bayesian network for multivariate probabilistic modelling of weigh-in-motion system data. Transp. Res. Interdiscip. Perspect. 13, 100552. http://dx.doi.org/10.1016/j.trip.2022.100552, URL: https://www.sciencedirect.com/science/article/pii/S259019822200015X.

Min, A., Czado, C., 2010. Bayesian inference for multivariate copulas using pair-copula constructions. J. Financ. Econom. 8, 511–546. http://dx.doi.org/10.1093/jfinec/nbp031.

Morales Napoles, O., 2010. Bayesian Belief Nets and Vines in Aviation Safety and Other Applications (Ph.D. thesis). TU Delft.

Morales Napoles, O., 2016. About the number of vines and regular vines on n nodes. http://dx.doi.org/10.13140/RG.2.1.4400.8083.

Morales-Nápoles, O., Hanea, A., Worm, D., 2014. Experimental results about the assessments of conditional rank correlations by experts: Example with air pollution estimates. In: Safety, Reliability and Risk Analysis: Beyond the Horizon - Proceedings of the European Safety and Reliability Conference. ESREL 2013, shers, pp. 1359–1366.

Morales-Nápoles, O., Steenbergen, R., 2014. Analysis of axle and vehicle load properties through Bayesian networks based on weigh-in-motion data. Reliab. Eng. Syst. Saf. 125, 153–164. http://dx.doi.org/10.1016/j.ress.2014.01.018.

Morales Napoles, O., tno, r., 2014. Large-scale hybrid Bayesian network for traffic load modeling from weigh-in-motion system data. J. Bridge Eng. 20, http://dx.doi.org/10.1061/(ASCE)BE.1943-5592.0000636.

Müller, S., Schüler, L., Zech, A., Heße, F., 2022. GSTools v1.3: a toolbox for geostatistical modelling in python. Geosci. Model Dev. 15 (7), 3161–3182. http://dx.doi.org/10.5194/gmd-15-3161-2022, URL: https://gmd.copernicus.org/articles/15/3161/2022/.

Papaioannou, I., Straub, D., 2015. Computing the reliability of shallow foundations with spatially distributed measurements. In: Geotechnical Safety and Risk V. IOS Press, pp. 958–963.

Paprotny, D., Kreibich, H., Morales Napoles, O., Wagenaar, D., Castellarin, A., Carisi, F., Bertin, X., Merz, B., Schröter, K., 2021. A probabilistic approach to estimating residential losses from different flood types. Nat. Hazards 105, 1–33. http://dx.doi.org/10.1007/s11069-020-04413-x.

Paprotny, D., Morales Napoles, O., 2017. Estimating extreme river discharges in Europe through a Bayesian network. Hydrol. Earth Syst. Sci. 21, 2615–2636. http://dx.doi.org/10.5194/hess-21-2615-2017.

Paprotny, D., Morales-Nápoles, O., Worm, D.T., Ragno, E., 2020. BANSHEE–A MATLAB toolbox for non-parametric Bayesian networks. SoftwareX 12, 100588. http://dx.doi.org/10.1016/j.softx.2020.100588, URL: https://www.sciencedirect.com/science/article/pii/S2352711020303010.

Pouliasis, G., Torres-Alves, G.A., Morales-Napoles, O., 2021. Stochastic modeling of hydroclimatic processes using vine copulas. Water 13 (16), http://dx.doi.org/10.3390/w13162156, URL: https://www.mdpi.com/2073-4441/13/16/2156.

Rasmussen, N.S., 1997. Concrete immersed tunnels — Forty years of experience. Tunn. Undergr. Space Technol. 12 (1), 33–46. http://dx.doi.org/10.1016/S0886-7798(96)00061-2, URL: https://www.sciencedirect.com/science/article/pii/S0886779896000612.

RWS, 2017. Richtlijn Ontwerp Kunstwerken v1.4. Ministerie van Infrastructuur en Milieu.

Soubra, A.-H., Youssef Abdel Massih, D., Kalfa, M., 2008. Bearing capacity of foundations resting on a spatially random soil. GeoCongress 2008 66–73. http://dx.doi.org/10.1061/40971(310)8.

van Tongeren, H., 1978. The foundation of immersed tunnels. In: Proceedings of Delta Tunneling Symposium. pp. 48–57.

Torres-Alves, G., 't Hart, C., Morales-Nápoles, O., Jonkman, S., 2022. Structural reliability analysis of a submerged floating tunnel under copula-based traffic load simulations. Eng. Struct. 269, 114752. http://dx.doi.org/10.1016/j.engstruct.2022.114752, URL: https://www.sciencedirect.com/science/article/pii/S0141029622008409.

Vanmarcke, E., Shinozuka, M., Nakagiri, S., Schuëller, G., Grigoriu, M., 1986. Random fields and stochastic finite elements. Struct. Saf. 3, 143–166. http://dx.doi.org/10.1016/0167-4730(86)90002-0.

Vatter, T., Nagler, T., 2022. Pyvinecopulib 0.6.1. URL: https://vinecopulib.github.io/pyvinecopulib/.

Virtanen, P., Gommers, R., Oliphant, T., Haberland, M., Reddy, D., Burovski, E., Peterson, P., Weckesser, W., Bright, J., van der Walt, S., Brett, M., Wilson, J., Millman, K., Mayorov, N., Nelson, A., Jones, E., Kern, R., Larson, E., Carey, C., Polat, İ., Feng, Y., Moore, E., VanderPlas, J., Laxalde, D., Perktold, J., Cimrman, R., Henriksen, I., Quintero, E., Harris, C., Archibald, A., Ribeiro, A., Pedregosa, F., van Mulbregt, P., SciPy 1.0 Contributors, 2020. SciPy 1.0: Fundamental algorithms for scientific computing in python. Nature Methods 17, 261–272. http://dx.doi.org/10.1038/s41592-019-0686-2.

Yu, X., Cheng, J., Cao, C., Li, E., Feng, J., 2019. Probabilistic analysis of tunnel liner performance using random field theory. Adv. Civ. Eng. 2019, 1–18. http://dx.doi.org/10.1155/2019/1348767.